JND in friction

Human Threshold for Perceiving Changes in Friction when Combined with Linear System Dynamics

R. Veldhuis

TU Delft

Image by Jorgen Hendriksen from *https://unsplash.com/photos/7uu-sbnqCo4* (Unsplash License)

JND in friction

Human Threshold for Perceiving Changes in Friction when Combined with Linear System Dynamics

by

R. Veldhuis

to obtain the degree of Master of Science
at the Delft University of Technology,
to be defended publicly on Wednesday March 16, 2022 at 1:00 PM.

Student number:	4138570	
Project duration:	October 1, 2020 – march 16, 2022	
Thesis committee:	Prof. dr. ir. M. Mulder,	TU Delft, Supervisor
	Dr. ir. M. M. van Paassen,	TU Delft, Supervisor
	Dr. ir. D. M. Pool,	TU Delft, Examiner
	Dr. ir. J. de Winter,	TU Delft, Examiner

An electronic version of this thesis is available at http://repository.tudelft.nl/.

TU Delft

Preface

This work presents a research project into the *just-noticeable difference in friction when combined with linear system dynamics*. This research has been conducted as part of the requirements for obtaining my MSc in Aerospace Engineering at the TU Delft.

I would like to take the chance here to express my gratitude to the people who have assisted me in making this report into something that I can be proud of. First of all, I would like to thank my supervisors René van Paassen and Max Mulder. René for helping me have a seamless experience using the DUECA software and always being available for weekly meetings. Max I would like to thank for his thorough reading of my work which has helped me tremendously in improving the readability and quality of this thesis.

Also, I would like to thank everyone taking the time to participate in the experiment, with a very special thanks to Dirk van Baelen who had to drive quite a distance to Delft. Many thanks also to Wei Fu for his extensive work on just-noticeable differences laying the groundwork for the research presented here.

Finally, I would like to thank Laura for being the most loving and supporting girlfriend I can wish for. Having cooked and prepared most of my meals while working on this thesis her impact on the final product can not be overstated.

R. Veldhuis
Delft, March 2022

Contents

Research Paper

Human Threshold for Perceiving Changes in Friction when Combined with Linear System Dynamics

Robbin Veldhuis
Control and Simulation
Aerospace Engineering, TU Delft
Delft, Netherlands
R.Veldhuis@student.tudelft.nl

***Abstract*—Understanding human perception of haptic feedback is critical when designing and regulating these control systems. In recent years, experiments have been conducted to determine the Just-Noticeable Difference (JND) in mass-spring-damper dynamics using a hydraulic admittance display in the form of a side-stick. These experiments have resulted in a model of JNDs when interacting with linear second-order dynamics. In real-world applications, however, control force dynamics also commonly include nonlinearities like friction. This research extends the current understanding of JNDs in linear systems by including the nonlinear case, where friction is also present. Experiments were conducted to determine JNDs in friction when combined with second-order system dynamics. Initial results suggest that friction JND can be independent of linear system dynamics as long as its value compared to the linear system's impedance is sufficiently large. This means, friction JND follows Weber's law, also when it is combined with mass-spring-damper dynamics, unless the level of friction approaches the detection threshold, which in turn can be influenced by the linear system dynamics. Based on the findings presented, it is possible to conduct more focused experiments to confirm and add to these initial results.**

***Index Terms*—JND, friction, mass-spring-damper system, masking, perception, human threshold**

I. Introduction

In manual control tasks where no direct link exists between the human control output (force) and the dynamical system being manipulated, haptic feedback becomes essential [1]. The benefits of this disconnect, however, are plentiful. Not only can haptic feedback be adjusted or extended to accommodate more intuitive control of complex dynamical systems, it is also possible to physically move the human controller to a different location, allowing for teleoperation [2]–[4]. In flight simulation, force-feedback combined with reliable models of control force dynamics can help pilots develop the proper muscle memory in training.

Due to inacuracies in the force-feedback, resulting from limitations in Control Loading System (CLS) hardware and software as well as imperfect modeling of the control forces, haptic displays may never reach perfect transparency [5]. However, when applying a human-centric approach to haptic display design and considering the limited resolution of human perception, achieving perfect transparency becomes a futile pursuit.

The thresholds for perceiving changes in haptic feedback, and indeed for perceiving changes in many other quantities as well, follow the relationships for Just-Noticeable Differences (JNDs) formulated by Weber. In human-centric design, the required transparency of haptic displays follows from knowledge of these JNDs. This means it is unnecessary to aim for haptic display transparency beyond a level at which further improvement is imperceivable.

The Weber-Fechner Law states that JNDs will be a fraction of the reference stimulus intensity [6] and Jones et al. showed that this law of JNDs applies to force-feedback for dynamical systems when looking at system properties in isolation, in this case studying the perception of stiffness [7] and viscosity/damping [8]. However, Rank et al. [9], among others, showed that in systems where these properties like stiffness and damping act simultaneously, as in for example mass-spring-damper systems, there is an interaction between them that determines the individual JNDs. Because mass-spring-damper systems are very common in manual control systems these interactions are of much interest in the study of force-feedback JNDs.

Fu et al. [10] studied this problem and formulated a unifying model for JNDs in linear system dynamics. This model extends Weber's law and under the assumption that humans use a test input with a dominant frequency, states that the JNDs for stiffness, mass, or damping are proportional to the magnitude of the frequency response function of the complete system, which can then be generalized to higher-order systems [10]. But where the model of Fu et al. only deals with linear systems, Coulomb friction is a non-linear component relevant in many control tasks, particularly for the CLS of flight and helicopter simulators [11].

Gueorguiev et al. [12] studied the JND in friction, in isolation, and found constant Weber fractions for Coulomb friction. Messaoud et al. [13] confirmed these results. Because Coulomb friction is defined as a constant force opposing the direction of movement at nonzero velocity it can indeed be expected to follow the Weber-Fechner Law. Possibly because this research on friction JNDs focused on tactile perception of touch displays, where friction accounts for most of the haptic feedback, there is currently an absence of research on friction JND in the presence of mass-spring-damper dynamics as found in most flight control sticks.

This paper aims to build upon Fu's unifying JND model [10] and extend it to the nonlinear case by adding friction. Two fundamental research questions need to be addressed for this model extension:

1) *What is the friction JND in the presence of second-order system dynamics?*
2) *How does friction, when added to a second-order system, affect the stiffness, mass and damping JNDs?*

The research presented focuses on the first question and aims to identify all properties of the mass-spring-damper system that affect the friction JND. Furthermore, a first hypothesis is formulated of a model of friction JNDs in the presence of second-order dynamics.

The paper is structured as follows. After a brief introduction, Section II describes the problem in more detail, presents some of the initial analyses, and proposes an experiment. Section III explains the methodology behind the experiment, followed by its results in Section IV. Results are discussed in Section V, Section VI concludes the paper.

II. Background

A. JND for second-order dynamics

The study of JNDs in friction in the presence of second-order system dynamics will be conducted by taking the most relevant research available as a basis from which analyses will be performed and hypotheses formulated. This previously conducted research dealt with JND masking effects within linear systems, most notably JND experiments performed by Fu et al. [10] as well as Caldiran et al. [14]. Both investigated the masking problem by studying it in the frequency domain. This means determining JNDs in the real or imaginary parts of the Frequency Response Function (FRF) of a given system (Fu et al.), or JNDs in its magnitude and phase response (Caldiran et al.).

Given a general second-order system $H(j\omega)$, with $\Delta\Re H(j\omega)_{jnd}$ and $\Delta\Im H(j\omega)_{jnd}$ as the JND in the real and imaginary parts of the system's FRF respectively, the unified JND model formulated by Fu et al. is given by:

$$\frac{\Delta\Re H(j\omega)_{jnd}}{|H(j\omega)|} \approx \frac{\Delta\Im H(j\omega)_{jnd}}{|H(j\omega)|} = constant. \tag{1}$$

Since the real part of the system's FRF consists of the in-phase components of its impedance, $\Delta\Re H(j\omega)_{jnd}$ is the *coupled* JND in stiffness k and mass m, see Eq. (2). The out-of-phase, imaginary part of the system's response $\Delta\Im H(j\omega)_{jnd}$ is the JND in damping b, as shown in Eq. (3).

$$\Delta\Re H(j\omega)_{jnd} = \Delta k_{jnd} - \Delta m_{jnd} \cdot \omega^2 \tag{2}$$

$$\Delta\Im H(j\omega)_{jnd} = \Delta b_{jnd} \cdot \omega \cdot j \tag{3}$$

Using Fu's model the individual JNDs in stiffness, mass and damping can be expressed as a function of the system's initial stiffness, mass, damping as well as the excitation frequency ω. When drawing a system's response in the complex plane, this JND model states that a region can be defined, proportional in size to its magnitude response, inside which changes to the system fall within the JND and will therefore not be perceived by a human operator.

Caldiran et al. [14] conducted experiments where JNDs in firmness and bounciness were studied, which correspond to JNDs in the magnitude response of the second-order system or its phase response respectively. It should be noted that whereas Fu et al. used a side-stick, controlled by an electro-hydraulic motor, for the haptic feedback, Caldiran studied the JNDs for pressing a surface with a single finger using a Phantom Premium 1.0 device for the haptics. From their experiments, Caldiran found that the JND in magnitude response of the system was independent of the phase, whereas the JND in the phase response was monotonically increasing.

Combining the results from both researches, it is possible to hypothesize on the actual shape of the region of no change in perception, when representing a mass-spring-damper system in the complex plane. As discussed by Fu this region could be either elliptical or circular [10], but for the practical application of a unified JND model for CLS design, this may not be relevant. Current requirements on CLS transparency as given by EASA [15] or the FAA [16] are quite stringent and do not consider the limits of human perception, therefore implementing even the most conservative model of human perception (using the lowest JNDs) would be a considerable step in improving the match between device requirements and human perceptual capabilities.

B. Equivalent linear system analysis

As stated before, friction is considered an important part of the haptic feedback of most CLS designs. Especially for helicopter simulation but also for fixed-wing aircraft, friction accounts for a significant proportion of the control forces [11]. Currently, the research on JNDs in friction is very limited and when available it only considers friction on tactile displays [12], [13], [17], [18]. When considering the perception of friction while sliding a finger across a surface, mechanoreceptors in the skin may play an important role [18] and therefore the results may not translate well to the perception of flight stick impedance. Research conducted by Gueorguiev et al. [12] (using a tactile display) found constant Weber fractions for JNDs in friction, consistent with earlier research into stiffness and damping JNDs [7], [8]. The research in this paper, however, considers the potential masking effects of stiffness, mass and damping on the friction JND and no literature was found discussing this specific topic.

Considering Coulomb friction, for a mass-spring-damper system with friction added, the system dynamics can be described in the time domain as follows:

$$m\ddot{x}(t) + b\dot{x}(t) + f\,\mathrm{sign}(\dot{x}(t)) + kx(t) = F(t) \tag{4}$$

$F(t)$ represents the force (or torque) resulting from a displacement $x(t)$, f the friction coefficient and $\text{sign}()$, the signum function, defined as:

$$\text{sign}(\Box) = \begin{cases} -1 & \Box < 0 \\ 0 & \Box = 0 \\ 1 & \Box > 0 \end{cases} \tag{5}$$

Considering a harmonic excitation of the system of Eq. (4), the contributions of the spring, mass, damper and friction (exaggerated friction for clarity) to the impedance are illustrated in Fig. 1. The analysis is performed calculating the force $F(t)$ (impedance) as a result of the excitation $x(t)$ because the control tasks considered in this paper are displacement (excitation) tracking tasks.

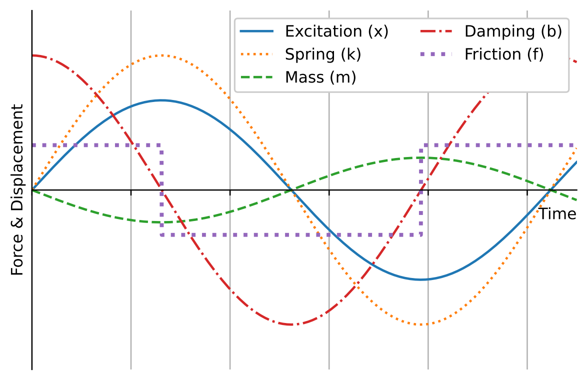

Fig. 1. Individual contributions from mass-spring-damper parameters, as well as friction, to the system's impedance when harmonically excited.

Equivalently to the damping contributions, friction forces act out-of-phase to the harmonic excitation. When all the contributions in Fig. 1 are added, Fig. 2 can be constructed. The system including friction will be approximated linearly using two different methods. The maximum impedance model and the phase-shift model.

1) Maximum impedance model: When considering the system's total impedance to a harmonic excitation, one approach of approximating the system with friction linearly would be to increase the magnitude response of the linear system while keeping its phase response constant. Where this approach does not take into account the instantaneous changes in force occurring at the extremes of the excitation, it does deal with the increased amplitude of the impedance signal. The observation of increased magnitude and constant phase allows for defining the equivalent linear dynamics of a system including friction as visualized in Fig. 2.

These equivalent linear dynamics using the maximum impedance model can be described as:

$$|H(j\omega)|_{eq} = |H(j\omega)| + f, \quad \angle H(j\omega)_{eq} = \angle H(j\omega) \tag{6}$$

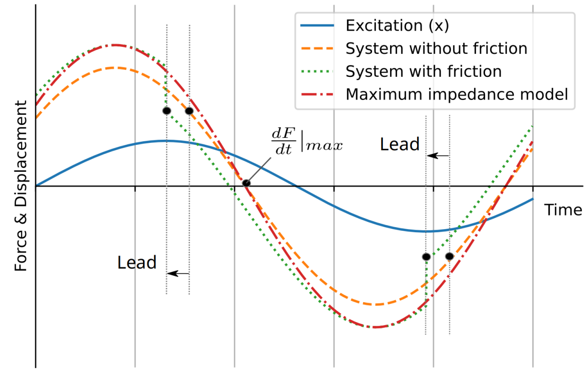

Fig. 2. Impedance of mass-spring-damper system including and excluding friction, illustrating the equivalent linear dynamics using the maximum impedance model.

Here, $H(j\omega)$ represents the original mass-spring-damper system and f the friction force (or torque when considering rotational stick motion).

2) Phase-shift model: The maximum impedance model approximates the nonlinear system with friction quite well at the extremes of the impedance, but for the regions in between it is far from accurate. In these regions, the system with friction can be best approximated by introducing a phase-lead to the linear frictionless system, which makes sense from the earlier realization that friction, like damping, acts out of phase. This phase shift, as caused by friction and visualized as a phase-lead in Fig. 2, can be determined by shifting the original linear system over the x-axis until it intercepts the system with friction at the crossing of the x-axis. Defining the excitation (displacement) as:

$$x(t) = \sin(\omega t) \tag{7}$$

The impedance $F(t)$ follows from the magnitude and phase response of the second-order system:

$$F(t) = |H(j\omega)| \sin(\omega t + \angle H(j\omega)) \tag{8}$$

Now the derivative of force with respect to time dF/dt is given by:

$$\frac{dF}{dt} = |H(j\omega)| \cdot \omega \cdot cos(\omega t + \angle H(j\omega)), \tag{9}$$

Realizing that at the moment of crossing the x-axis dF/dt is at its maximum, dF/dt at the x-axis crossings is defined as:

$$\frac{dF}{dt}|_{max} = |H(j\omega)| \cdot \omega \tag{10}$$

Since the difference in force between both systems, with or without friction, at any given time will be due to the friction force f. The shift in time, t_{shift} is then given by:

$$t_{shift} = f \cdot \frac{dt}{dF} = \frac{f}{|H(j\omega)| \cdot \omega} \tag{11}$$

The corresponding phase shift ϕ_{shift} is given by:

$$\phi_{shift} = \omega \cdot t_{shift} = \frac{f}{|H(j\omega)|} \tag{12}$$

Fig. 3 illustrates the equivalent linear dynamics, applying the phase-lead as described. The approximation matches the nonlinear system with friction only in the regions between maximum impedance.

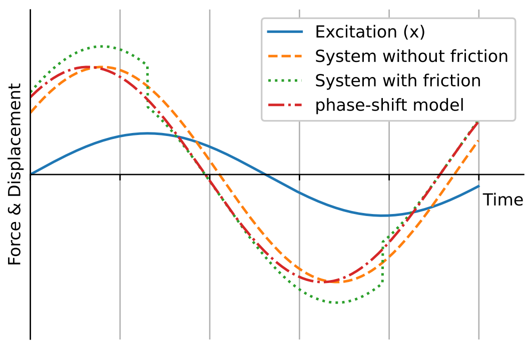

Fig. 3. Visualization of impedance of mass-spring-damper system including and excluding friction, illustrating the equivalent linear dynamics using the phase shift model where $\angle H(j\omega) < \pi/2$ and thus a phase-lead is applied.

The phase-lead from this equivalent dynamics phase-shift model becomes a phase-lag when the original linear system's response $\angle H(j\omega)$ has a phase $\phi > \frac{\pi}{2}\ rad$, as illustrated by Fig. 4.

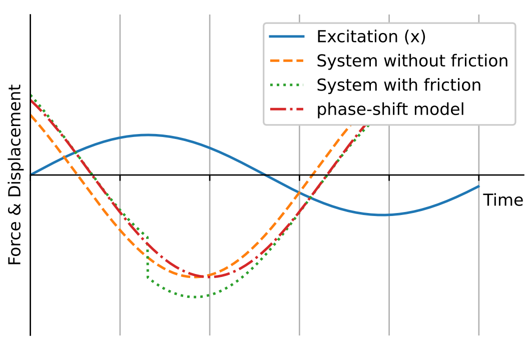

Fig. 4. Visualization of impedance of mass-spring-damper system including and excluding friction, illustrating the equivalent linear dynamics using the phase shift model where $\angle H(j\omega) > \pi/2$ and thus a phase-lag is applied.

Where this phase response is determined by the linear system's parameters (stiffness k, damping b, mass m) and excitation frequency ω. The equivalent dynamics phase-shift model changes back and forth between a phase-lead and a phase-lag every $\phi = k \cdot \frac{\pi}{2}$ (with $k = 0, 1, 2..$) as illustrated in Fig. 5. Furthermore, at the regions of $\phi = k \cdot \frac{\pi}{2}$, the phase shift approximation breaks down and the system with friction would be better approximated by alternating a phase-lead and a phase-lag at two times the excitation frequency.

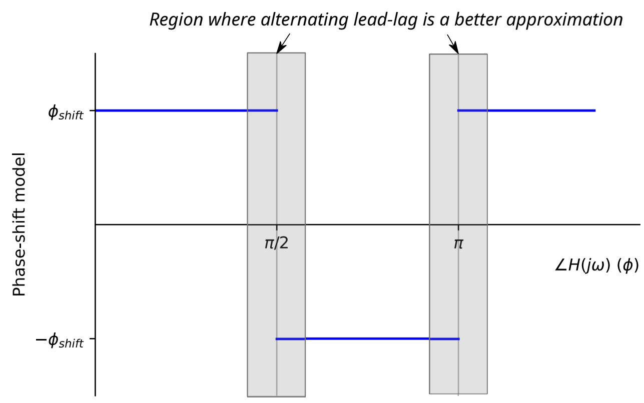

Fig. 5. Equivalent dynamics phase-shift model visualization as a function of the second-order system's phase response (note $\angle H(j\omega)$ is a function of ω as well).

However, the purpose of this study is not to find the best linear approximation of a system including friction, but the linear approximation is just one of the tools used to construct hypotheses of JNDs in friction and analyse experiment results. Therefore, in this paper's consideration of equivalent dynamics, only systems (and excitation frequencies) with phase response $0 < \phi < \frac{\pi}{2}$ are considered.

Given both equivalent linear dynamics models, it is possible to apply Fu's theory and hypothesize about the role of second-order dynamics on friction JNDs. Where Fu described the JND in the real and imaginary parts of a second-order system's FRF, changes in the real and imaginary part of a system can also be described by a simultaneous change in magnitude response and phase. In the perception of dynamical systems, both motion x and force F cues play an important role. Together, these cues can be combined to distinguish different springs or dampers. Fu et al. [19] performed an experiment where the relationship between these two cues was studied by performing JND measurements of spring stiffness. They found that when controlling for force – by having subjects apply the same force on different springs resulting in different displacements – JNDs in spring stiffness were higher when compared to controlling for displacement (where the displacement was constant and the different force was the main cue). This experiment shows that without visual feedback, the displacement can be difficult to use as a cue for discriminating stiffnesses. From these findings, it is possible to hypothesize that the increased *magnitude*, as caused by adding friction to a linear system, is of more importance than the apparent phase changes in discriminating levels of friction when no visual feedback is available. However, when there is a clear visual displacement cue, which is necessary for analyzing JNDs in the frequency domain (requiring a constant harmonic excitation which can be induced by a preview tracking task), a changed phase response may equally contribute. Additionally, when discussing the region of no noticeable difference, expressed around the FRF in the complex plane (visualized in Fig. 6), Fu hypothesized [10] it could be circular, which would imply a great sensitivity also for a change purely in the phase response.

Taking this into consideration, both approaches of equivalent linear dynamics (maximum impedance model and phase-shift model) could be relevant in exploring JNDs in friction from the perspective of Fu's JND model. For a second-order system with a phase response $0 < \phi < \frac{\pi}{2}$ the time domain response of the equivalent linear dynamics system combining both models is plotted in Fig. 7 as well as both models' frequency responses in the complex plane in Fig. 6. The visualization in the time domain follows from a system alternating between an increased magnitude response and a phase-lead at four times the excitation frequency, but what is most important to recognize is that for the systems discussed, the two modes alternating does approach the nonlinear system reasonably well. Therefore, these two modes of linear approximations could play a role in the perception of friction as well as the threshold for perceiving changes in friction, and Fu's JND model can be applied to both modes.

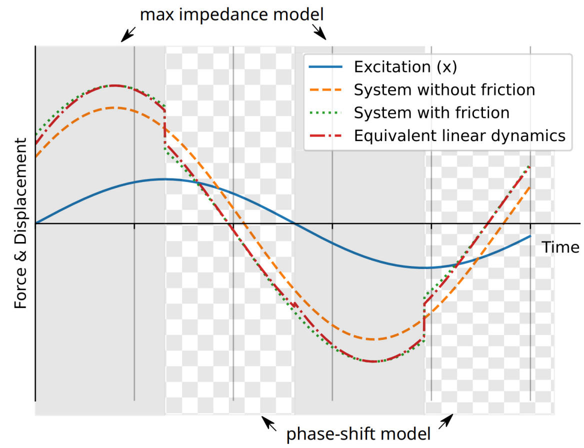

Fig. 7. Visualization of impedance of mass-spring-damper system including and excluding friction, illustrating the combined equivalent linear dynamics by alternating the maximum impedance model and phase-shift model.

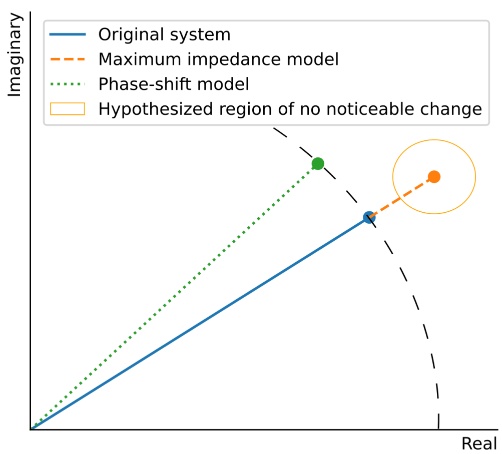

Fig. 6. Complex plane representation of equivalent linear dynamics, showing both maximum impedance and phase-shift models while indicating the region of no noticeable change according to Fu et al. [10].

C. Perception of the nonlinear

This approach of finding equivalent linear dynamics does not deal with a very important part of the perceived forces due to friction, which is the nonlinear force change itself, occurring at the moment of direction change. This sudden change in force, or force-drop, cannot be described using second-order dynamics. Nonetheless, this drop may be, consciously or subconsciously, perceived and compared when distinguishing different levels of friction. Weber's law defines the threshold for perceiving changes in force, the JND, as the constant portion of the reference force from which the change occurs [20]. This law holds over a wide range of sensory modalities and only breaks down in the regions where the stimulus intensity is close to the detection threshold [21], where the JND is no longer a constant portion of the reference stimulus intensity but increases.

A possible hypothesis for friction JNDs in the presence of second-order dynamics is that the force-drop is used for the perception of friction independently of other dynamics. For friction when perceived in isolation, the little available research shows Weber's law to hold, but this could well be due to the perception of a constant force when moving in one direction. When other forces due to interactions with mass-spring-damper dynamics are present, this friction force may be more difficult to distinguish. Nevertheless, the force-drop itself could still be used in the perception and even the perception of differences (or JNDs). If this force-drop is perceived, as a stimulus above some detection threshold, then it is possible that a mass-spring-damper system has no influence on the friction JND and it is only proportional to reference friction. *In other words, the change in force-drop that is just perceivable is then a constant fraction of the reference force-drop.*

The main properties that are expected to influence the force-drop perception are the real part of the second-order system $\Re H(j\omega)$, its phase $\angle H(j\omega)$ and the excitation frequency ω. The real part $\Re H(j\omega)$ is responsible for the force occurring at the extremes of the excitation, because the velocity is always zero at this point and damping plays no role here. If the perception of the force-drop itself follows Weber's law, then for an equal change in force, the force from which this change occurs (the reference force) determines whether the change is perceived. In other words, when the real part $\Re H(j\omega)$ is relatively large, the instantaneous force change occurring at the extremes of the excitation may be less likely to be perceived compared to a smaller $\Re H(j\omega)$ (where $\Re H(j\omega)$ is affected by the second-order system mass m and stiffness k). The effect of $\Re H(j\omega)$ on the force-drop is illustrated in Fig. 8.

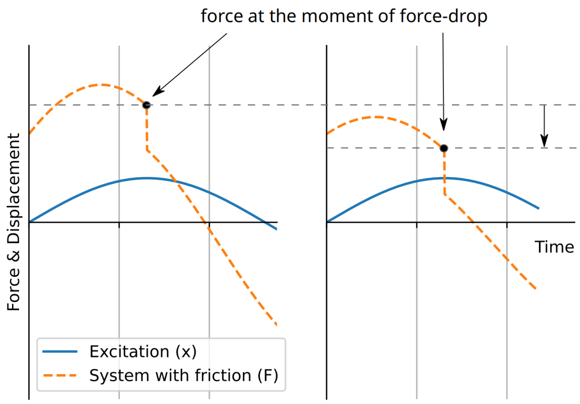

Fig. 8. The effect of lowering $\Re H(j\omega)$ on the force at the moment of the force-drop caused by friction.

Decreasing $\Re H(j\omega)$ also causes a shift of the phase at which the force-drop occurs. Since the force-drop can be described as the derivative of force with respect to time dF/dt reaching infinity, when this drop in force coincides with a large value for dF/dt of the system's impedance, there could be a masking effect that is not present at lower dF/dt levels. Reasoning in a similar way then explains the potential effect of the excitation frequency on the perception of the force-drop, as both frequency and phase can influence the value of dF/dt at the moment of the force-drop (as seen in Fig. 9). The excitation frequency ω scales dF/dt (Eq. (9) shows ω as a scaling factor) while $\angle H(j\omega)$ determines the phase at which the force-drop occurs (and therefore indirectly affects dF/dt). Fig. 9 illustrates how the excitation frequency can potentially mask the force-drop by scaling dF/dt.

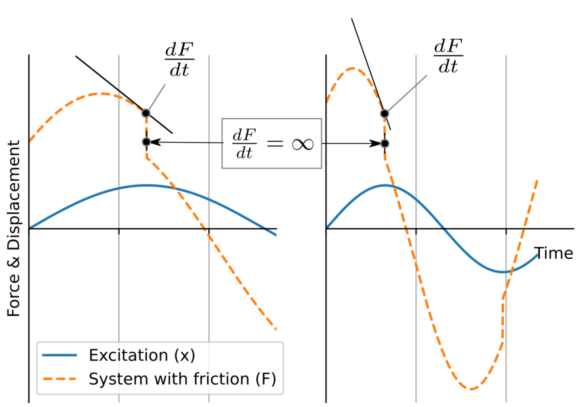

Fig. 9. The effect of increasing the excitation frequency ω on the dF/dt at the moment of the force-drop caused by friction.

D. Hypotheses

Based on the analysis and recent research, it is possible to construct several hypotheses on the JND in friction when it is presented together with mass-spring-damper dynamics. The most simple hypothesis assumes no masking effect of the second-order system on friction:

1) **Friction JND is proportional to the reference friction setting, independent of mass-spring-damper parameters.**

This would be the case if the friction is perceived independently of other dynamics, most likely due to the nonlinear changes in force playing a big role in perception. When this first hypothesis holds, friction JNDs are expected to be constant fractions of the reference friction, satisfying Weber's law, as previous research into friction JNDs without potential masking dynamics indicates [12], [17].

For the scenario when some form of masking occurs due to the mass-spring-damper system, the analysis of linear equivalent dynamics can be applied to Fu's JND model to construct a second hypothesis. Using the description of equivalent dynamics, both the maximum impedance and phase-shift models of equivalent dynamics result in a hypothesis of the friction detection threshold, as well as the JND. To be able to detect friction, the euclidean distance between the two different modes of equivalent dynamics in the complex plane should be larger than the region of no noticeable change. This is illustrated in Fig. 6. Then, considering the JND, for a difference in friction to become noticeable, it needs to fall outside of the detection threshold of the equivalent dynamics system including friction, meaning the JND in friction would be close to the detection threshold, with the detection threshold depending on the second-order system settings. The second hypothesis can be formulated as follows:

2) **The friction JND follows from Fu's JND model, where JNDs in friction are proportional to the magnitude response of the equivalent linear system.**

Also discussed in the analysis, is the possibility that the instantaneous force-drop in the system response plays an important role in the perception of friction and changes in friction. Factors that have been identified to potentially mask the perception of this force-drop are $\Re H(j\omega)$, $\angle H(j\omega)$ as well as the excitation frequency ω. Therefore, because $\angle H(j\omega)$ and $\Re H(j\omega)$ are coupled, and for a constant magnitude response can not be considered in isolation, the third and final hypothesis is:

3) **The friction JND is influenced by second-order system excitation frequency or system phase response independently of its magnitude response.**

E. Experiment Conditions

The hypotheses formulated will be tested in an experiment, discussed in more detail in Section III, where the influence of mass-spring-damper dynamics on friction JND will be studied. To study these effects, the JNDs should be established for several conditions of second-order system parameters and

TABLE I
EXPERIMENT CONDITIONS

Condition	$\|H(j\omega)\|$	$\angle H(j\omega)$ [rad]	$\Re H(j\omega)$	$\Im H(j\omega)$	k [Nm/rad]	m [kg]	b [Nms/rad]	ω [rad/s]	f [Nm]
1	2.12	0.79	1.5	1.5	1.87	0.01	0.25	6	0.1
2	2.12	0.79	1.5	1.5	1.87	0.01	0.25	6	0.15
3	2.12	0.79	1.5	1.5	1.87	0.01	0.25	6	0.2
4	1.6	0.79	1.13	1.13	1.49	0.01	0.19	6	0.15
5	2.6	0.79	1.84	1.84	2.2	0.01	0.31	6	0.15
6	2.12	1.02	1.10	1.81	1.74	0.01	0.23	8	0.15
7	2.12	0.40	1.95	0.83	2.04	0.01	0.28	3	0.15
8	2.12	1.02	1.10	1.81	1.46	0.01	0.3	6	0.15
9	2.12	0.40	1.95	0.83	2.31	0.01	0.14	6	0.15

reference friction settings. All details of these conditions are given by Table I and further discussed below.

Starting from the first hypothesis, stating that the perception of friction follows Weber's law and is not dependent on the second-order system dynamics, a set of three conditions (1, 2, 3) can be defined where the reference friction is varied and the second-order system $H(j\omega)$ stays constant. These experiment conditions are illustrated by Fig. 10, where for the indication of reference friction settings in the complex plane the maximum impedance model is used as given by Eq. (6) and illustrated in Fig. 6.

By varying the friction, it is possible to determine whether Weber's law holds for friction JNDs when constant mass-spring-damper dynamics are present. However, to properly test the first hypothesis, other settings of mass-spring-damper dynamics need to be considered as well, establishing if a masking effect is present. This variation of mass-spring-damper dynamics will be accomplished by combining the results of all following conditions.

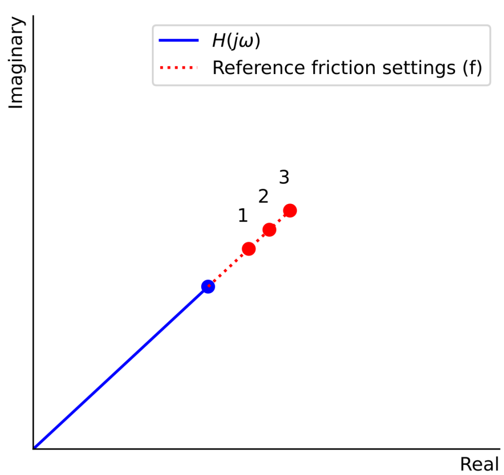

Fig. 10. Visualization of the first set of three conditions, with a constant $H(j\omega)$ and a varying reference friction (zoomed-in for clear distinction between friction settings).

To further test the first hypothesis, and also to investigate the second hypothesis, the friction JND is determined for different magnitude responses of the masking mass-spring-damper system $|H(j\omega)|$ while keeping the reference friction constant. Whether friction JND is indeed proportional to the magnitude response of the equivalent linear system dynamics $|H(j\omega)_{eq}|$ will be tested with this set of three conditions (4, 2, 5), illustrated in Fig. 11. To minimize the number of conditions, Condition 2 is reused to establish multiple series of three system settings for statistical analysis.

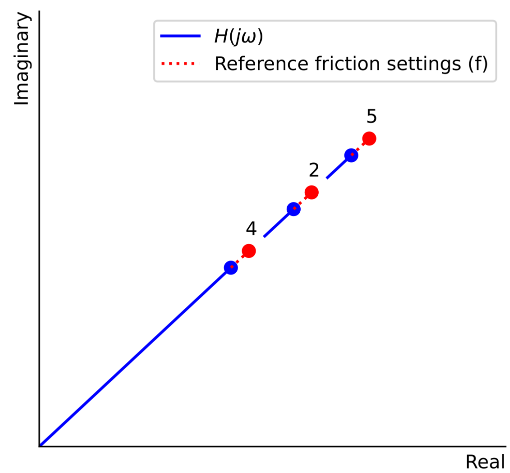

Fig. 11. Visualization of the second set of three conditions, where $|H(j\omega)|$ is varied while keeping the reference friction constant.

Finally, the third hypothesis considers the possibility that the second-order system's phase response or excitation frequency influences the friction JND. If this is indeed the case, varying both parameters while keeping the reference friction and $|H(j\omega)|$ constant should show an effect on friction JND. Therefore, in the final conditions that will be tested, three different second-order system phase responses $\angle H(j\omega)$ will be considered. In one series of three settings, $\angle H(j\omega)$ is adjusted by changing $\Re H(j\omega)$ and $\Im H(j\omega)$ while keeping $|H(j\omega)|$ constant (Conditions 8, 2, 9). For the other series of three settings, the excitation frequency ω is varied (Conditions 6, 2, 7). These last two sets of three conditions are illustrated in Fig. 12. Conditions 6 and 8, as well as 7 and 9, have been matched in phase response, so that differences in friction

JND due to excitation frequency not accounted for by phase differences can be studied. For example, when $\angle H(j\omega)$ affects the friction JND but the excitation frequency does not, then no difference should be found between Condition 6 and 8 or 7 and 9. If, however, excitation frequency affects friction JND independently of mass-spring-damper phase response, JNDs for Conditions 6 should differ from Condition 8 as should JNDs for Condition 7 from 9.

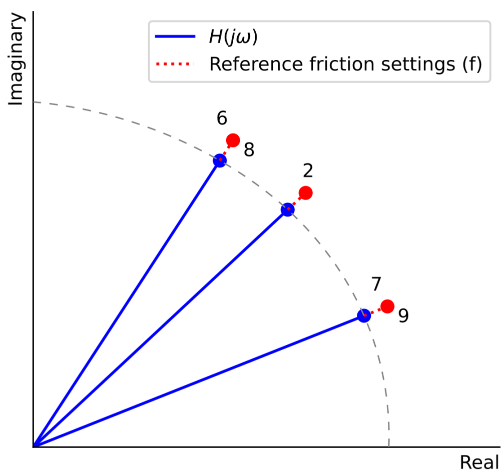

Fig. 12. Visualization of the third (6, 2, 7) and fourth (8, 2, 9) set of three conditions. It should be noted that conditions 6 and 8 as well as 7 and 9 have the same FRF but they differ by excitation frequency ω, which can be seen in Table I.

III. Method

A. Apparatus and Participants

The experiment was performed at the Human-Machine Interaction Laboratory at the Faculty of Aerospace Engineering (TU Delft, The Netherlands). The admittance controlled side-stick (right hand) manipulator presents the haptic feedback to participants and is driven by an electro-hydraulic motor. All visual cues were displayed on an 18" LCD screen $80\ cm$ in front of the subjects. For the conducted experiment, the side-stick was limited to 1-DoF, only able to move laterally (rolling left or right in flight control terms).

The experiment was approved by the Human Research Ethics Committee of the TU Delft (ID:1827) and involved nine participants, eight males and one female. Participants had no impairment of the right arm and during a 20-minute training, preceding the actual experiment, showed they were able to successfully perform the experiment tasks.

B. Experiment Setup and Procedure

With each participant, the friction JND was established for all nine conditions through an adaptive one-up/two-down staircase procedure [22], selecting one-up/one-down until the first reversal to realize faster convergence. The ratio between stepsize downwards and upwards was set at 0.5488, converging to a JND with an 80.35% correct performance [23]. The staircase automatically finished after the seventh reversal (change in direction of the staircase) or when reaching 40 trials. The last 4 reversals were averaged to calculate the JNDs. Four times in the entire experiment (81 staircases) did a staircase end with six reversals instead of seven, either due to reaching the limit of 40 trials or a program error. In these cases, it was chosen to select the last three trials to find the JNDs.

Similar to the experiments performed by Fu et al. [22], each step of the staircase presented the participant with two 6.3 s segments of a preview tracking task, with a tracking signal described by:

$$\theta_{ss} = 0.37 \cdot \sin(\omega t), \tag{13}$$

with θ_{ss} being the manipulator deflection angle in radians and ω the excitation frequency. The visual display also showed a progress bar at the top, indicating which of two trials was running. To accommodate a smooth transition, going from no movement to the $\omega\ rad/s$ excitation, the first and last seconds of the 6.3 s segments were used as a fade-in and fade-out phase, respectively. During these fade-in/fade-out phases, the amplitude of the sinusoidal displacement function was linearly interpolated (in time) between 0 and 0.37.

In terms of haptics, in each step, the subjects would be presented with a reference level of friction, as well as a comparatively higher level of friction, investigating the upper JNDs only. Then a two-alternative forced-choice method was used, with the subject having to indicate for which of the two trials the side-stick was perceived as having a "higher resistance to movement", resulting in feedback from participants that was either correct or false, leading to stepping up or down in the staircase procedure.

Participants were instructed and briefly trained to concentrate on following the tracking signal while still focusing part of their attention on perceiving the side-stick resistance. The experimenter would check, on a separate screen, whether the tracking task was followed with desirable accuracy and would give feedback on this performance if necessary.

To balance effects of learning and fatigue, a Latin square design was chosen. With nine participants and nine conditions, this equates to a 9x9 table (with a row for each participant giving the experiment condition order) where all conditions appear once in each row and each column.

C. Statistical Analysis

The measurement data from the experiment are in the form of friction levels at moments of reversal for every participant and every condition. With nine participants, the 81 available JNDs are calculated by averaging the friction levels of the last four out of seven reversals (or three when only six reversals are available). The JNDs are then corrected for between-subject variability, bringing the average of all nine JNDs for each participant to the average of all 81 JNDs of the

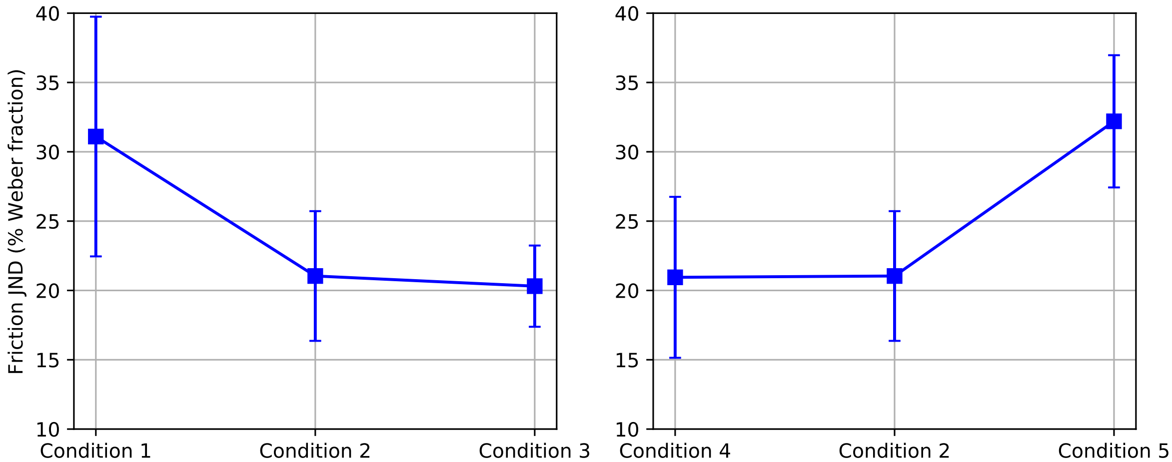

Fig. 13. Results of the first two sets of three experiment conditions (corresponding to Figs. 10 and 11), showing means and 95% confidence intervals for friction JND Weber fractions, with on the left-hand plot an increasing reference friction for a constant $H(j\omega)$ (Conditions 1, 2, 3), and on the right-hand plot an increasing $|H(j\omega)|$ for a constant reference friction (Conditions 4, 2, 5).

entire participant group. The 9x9 matrix is normalized to both reference friction and equivalent dynamics. After checking for sphericity using Mauchly's test, a one-way repeated-measures analysis of variance (ANOVA) is performed on several sets of conditions to determine the significance of potential masking effects of the second-order system on the friction JND, as well as effects of reference friction on friction JND.

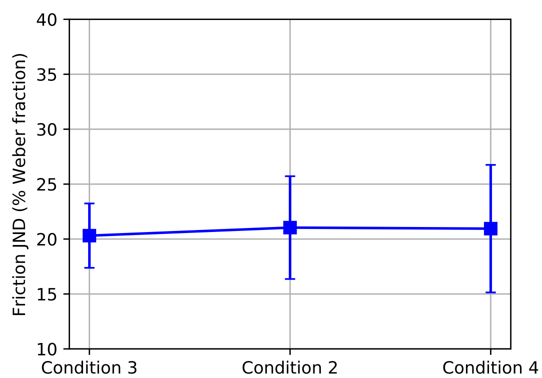

Fig. 14. Means and 95% confidence intervals of friction JND Weber fractions.

IV. Results

When taking the results of the first and second set of three conditions of the experiment (visualized in Fig. 10 and 11), Fig. 13 shows the means and 95% confidence intervals for the JNDs in friction. The JNDs are normalized to reference friction presenting Weber fractions on the vertical axis (in percentages) and the experiment conditions (corresponding to Table I) are given on the horizontal axis. The plot on the left of Fig. 13 shows the JNDs for a varying reference friction and a constant $H(j\omega)$ and the plot on the right shows the JNDs for constant reference friction and a varying $|H(j\omega)|$.

Fig. 13 shows that when plotting the friction JNDs as Weber fractions there seems to be a significant effect both from changing the reference friction setting (left-side of the figure) as well as from increasing the mass-spring-damper system magnitude response $|H(j\omega)|$ (right-side of the figure). Performing a one-way repeated measures ANOVA shows both effects are significant ($F(2, 16) = 6.42$, $p < 0.01$, for Conditions 1, 2 and 3 and $F(2, 16) = 4.37$, $p = 0.03$, for Conditions 4, 2 and 5).

Then, considering the hypotheses formulated in Section II-D it is clear that friction JND depends on mass-spring-damper dynamics, the first hypothesis is rejected. Friction JND is affected by the second-order system's magnitude response, as demonstrated by the results from Conditions 4, 2 and 5. Furthermore, for a constant second-order system, friction also does not seem to follow Weber's law, as can be seen from the results of Conditions 1 to 3.

The second hypothesis states that friction JND is proportional to the magnitude response of the equivalent linear system. From Fig. 13 it is clear that the effects of both reference friction and $|H(j\omega)|$ setting on friction JND are not linear, while these parameters do vary linearly between Conditions 1 to 3 and from Conditions 4, 2 to 5, respectively. Therefore, the second hypothesis is also, rejected.

When considering Conditions 2, 3 and 4 (Fig. 14) it shows that the Weber fractions are fairly constant ($F(2, 16) = 0.0262$, $p = 0.89$, sphericity assumption violated for this set of conditions and therefore Greenhouse-Geisser corrected p-value). In fact, just considering these conditions, the first hypothesis does seem to hold with JNDs in friction following Weber's law (Weber fractions of around 20%). For these three conditions, both reference friction as well as $|H(j\omega)|$ are varied, raising the question of how Conditions 1 and 5 actually differ. More specifically, what property do Conditions 1 and 5 share that they do not share with Conditions 2, 3 and 4? From Figs. 10 and 11, and further illustrated in Fig. 15, it can be seen that for these conditions, resulting in larger friction JNDs, friction is a relatively small proportion of the mass-spring-damper system magnitude response $|H(j\omega)|$. In other words, friction accounts for a smaller portion of the magnitude of the complete system's impedance. Hence, for the conditions with a constant phase response (here $\frac{\pi}{4}$ rad), the Weber fractions for friction JND will indeed be constant as long as the proportion of impedance magnitude accounted for by friction is large enough:

$$\frac{f}{|H(j\omega)|} > threshold \tag{14}$$

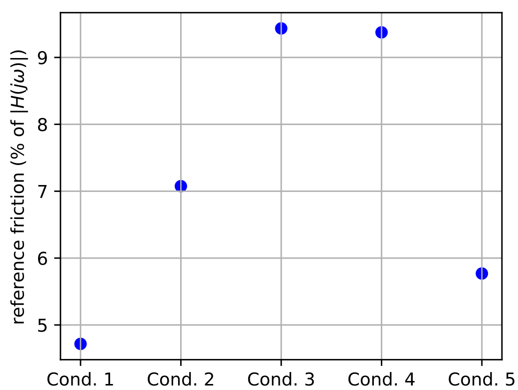

Fig. 15. The ratio of friction magnitude to second-order sytem magnitude response $f/|H(j\omega)|$ for Conditions 1 to 5.

The friction JND results for the third and fourth sets of conditions, illustrated in Fig. 12, are plotted in Figs. 16 and 17, respectively. These plots show the effects of excitation frequency ω and second-order system phase response $\angle H(j\omega)$ on friction JND, respectively.

Performing two one-way repeated measures ANOVA for sets of Conditions 6, 2, 7 (Fig. 16) ($F(2, 16) = 0.78, p = 0.48$) and 8, 2, 9 (Fig. 17) ($F(2, 16) = 0.52$, $p = 0.61$) shows no significant effects. However, a trend seems to be visible where the friction JND increases when the phase response $\angle H(j\omega)$ gets larger or smaller (from $\pi/4$ at Condition 2).

It was explained in Section II-E that conditions 6 and 8 as well as 7 and 9 can be compared to distuingish the effects of excitation frequency ω and phase response $\angle H(j\omega)$. Whether ω affects the friction JND independently from $\angle H(j\omega)$ is something that cannot be inferred from these results as the variances are simply too large to draw conclusions on the differences in means between Conditions 6 and 8 as well as 7 and 9. Paired samples t-tests demonstrate this lack of statistical significance comparing Condition 6 ($M = 27.6$, $SD = 13.2$) and Condition 8 ($M = 23.6$, $SD = 7.9$); $t(16) = 0.97$,

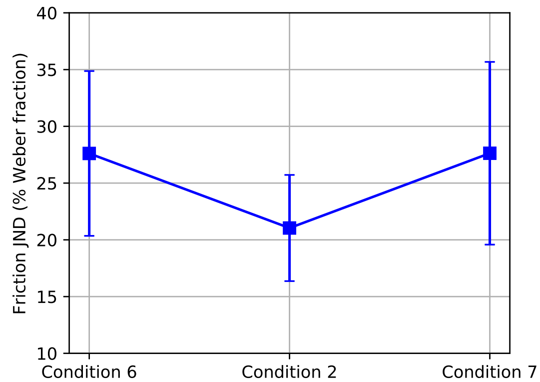

Fig. 16. Means and 95% confidence intervals of friction JND Weber fractions.

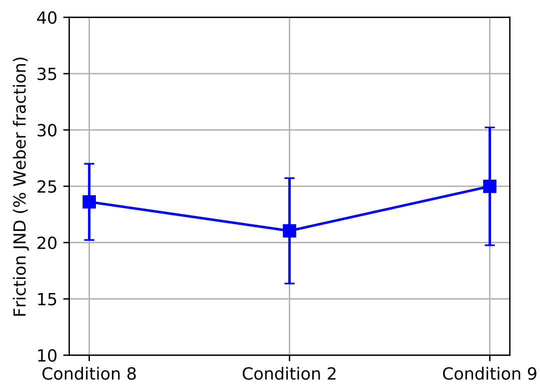

Fig. 17. Means and 95% confidence intervals of friction JND Weber fractions.

$p = 0.36$, as well as Condition 7 ($M = 27.6$, $SD = 12.6$) and 9 ($M = 25.0$, $SD = 10.0$); $t(16) = 0.48$, $p = 0.65$. However, it can be argued that increasing the excitation frequency, if having any effect at all, should increase the friction JND. This is because increasing ω, increases dF/dt at the moment of the force drop (as explained in Section II-C and visualized in Fig. 9). Therefore, the "v-shape" in Fig. 16 is unlikely to be caused by excitation frequency independent of $\angle H(j\omega)$, since Condition 7, with $\omega = 3\ rad/s$, should not result in a larger JND in friction than Condition 2, with $\omega = 6\ rad/s$. This makes the mass-spring-damper phase response the more likely cause of increased Weber fractions for friction JND in both sets of conditions (6, 2, 7 and 8, 2, 9).

V. Discussion

From the experiment results presented in the previous section, the first hypothesis, expecting JNDs in friction to follow Weber's law regardless of mass-spring-damper system setting, seems to hold for some conditions (Condition 2, 3 and 4 as illustrated by Fig. 14). Nevertheless, Conditions 1 and 5 show a significant effect of both reference friction and second-order system magnitude response $|H(j\omega)|$ on friction JND, respectively. One way of interpreting these increased Weber fractions is that they are caused by friction levels being closer to the detection threshold.

As noted in Section II and also discussed by Norwich [21], Weber's law has been shown to break down at the limits of perception, and it is possible that in our experiment these limits are affected by the mass-spring-damper dynamics. This means the second-order system dynamics do not directly influence the friction JND, but they do influence the detection threshold for friction and by raising that detection threshold, Weber fractions for friction JNDs will increase. An illustration of this phenomenon is given in Fig. 18.

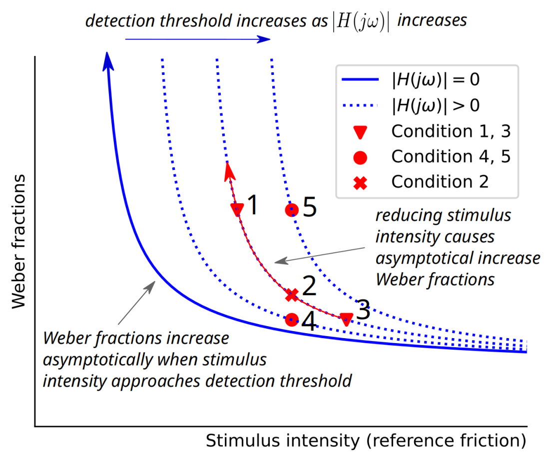

Fig. 18. Sketch of the asymptotic increase in Weber fractions of friction JND as a result of changing the reference friction (Conditions 1, 2, 3) or an increasing detection threshold as $|H(j\omega)|$ gets larger (Conditions 4, 2, 5). Both changing the reference friction, as well as increasing the detection threshold, show similar effects on the friction JND Weber fractions.

Considering the experiment results depicted in Fig. 13, Fig. 18 illustrates how varying the reference friction in the presence of constant second-order system dynamics (Conditions 1, 2, 3) leads to an asymptotic increase in Weber fractions for friction JND. Also, considering Conditions 4, 2 and 5, it can be observed that varying $|H(j\omega)|$ while keeping reference friction constant causes the same asymptotic increase in Weber fractions.

In Section II-B, using the equivalent linear dynamics theory, some suggestions have been made as to what the detection threshold depends on. It was hypothesized that either a change in equivalent linear dynamics magnitude or phase response, or a perception of the nonlinear force-drop, would determine whether friction is perceived or not. These hypotheses focused on friction JND rather than the detection threshold for friction. The same theory can nevertheless be applied to argue the validity of the suggestion expressed before (and visualized in Fig. 18) that the second-order system's magnitude response affects the friction detection threshold. Considering the levels of friction tested, it seems that the equivalent linear system dynamics increased magnitude and phase response cannot explain its perception fully. For example, a friction level of $0.15\ Nm$ is most likely well above the detection threshold in a system where $|H(j\omega)| = 2.12$ (from its JND Weber fraction in Fig. 14). However, applying Fu's JND model [10], the resulting equivalent magnitude and phase response changes from friction fall well within the detection threshold established by Fu:

$$\frac{f}{|H(j\omega)|} = \frac{0.15}{2.12} = 0.07 \tag{15}$$

Where Fu found Weber fractions of around 10%, the increased magnitude response due to friction is only around 7%. Then again, it is possible that the nonlinear force-drop occurring at a change in excitation direction is responsible for the perception of friction before the change in magnitude response plays any role. Where Fu had participants experience different mass-spring-damper system settings with a small break in-between trials, friction can be described by a sudden shift in system parameters within the trial itself. This difference could cause the Weber fractions to be lower, even if they still depend on $|H(j\omega)|$. Furthermore, when looking at the instantaneous change in equivalent linear system dynamics within a sinusoidal excitation, while applying Fu's JND model, it can be seen that this instantaneous change is actually larger than the level of friction. This is considering that the system including friction is best described in linear terms by a system "oscillating" between the earlier described maximum impedance model and the phase-shift model (Fig. 6). It was derived in Eq. (12) that the phase shift describing the instantaneous drop in force because of introducing friction is given by $f/|H(j\omega)|$. Using the small-angle approximation, it is found that the euclidean distance, on the complex plane, from the original frictionless system to the maximum impedance model system (which is the level of friction f as Eq. (6) indicates) is equal to the distance from the original system to the phase-shift model system, as illustrated in Fig. 19. Considering the angle between the original system and the phase-shift or maximum impedance model is approximately equal to $90\ deg$, the perceived instantaneous change in $\Re H(j\omega)$ due to friction is described by $\sqrt{2} \cdot f$. This is visualized in Fig. 19.

Now from these realizations and Fig. 19, together with the recognition that the size of the region of no noticeable change depends on $|H(j\omega)|$, which follows from Fu's JND model, a possible explanation is presented for $|H(j\omega)|$ affecting the detection threshold for friction. More data from additional experiments are needed to confirm these interpretations and to determine the exact relationship between the second-order system magnitude response and the detection threshold in friction. So where the results from this research show a connection between $|H(j\omega)|$ and friction JND, which are best explained by a change in detection threshold of friction, how this change in detection threshold occurs can only be hypothesized on.

When considering the results from the conditions studying the effect of excitation frequency ω and phase response $\angle H(j\omega)$, depicted in Fig. 16 and 17, no conclusions can be drawn that are backed by statistical significance. It is,

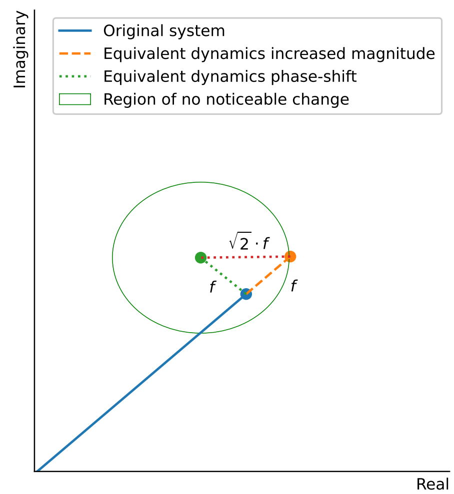

Fig. 19. Illustrating the instantaneous change in system dynamics on the complex plane with the region of no noticeable change derived from Fu's JND model. This example shows (zoomed in) experiment Condition 2.

nevertheless, possible to interpret the trends that are clearly visible in both figures. It was established in Section IV that there may be an effect of $\angle H(j\omega)$ on friction JND. This effect is visible in both excitation frequency conditions (6, 2, 7) as well as phase response conditions (8, 2, 9) and shows an increased friction JND for $\angle H(j\omega)$ increasing beyond $\pi/4$ as well as decreasing below $\pi/4$. In Section II it was argued that the phase response of the second-order system potentially affects the perception of friction, both due to changing the base level of force as well as the gradient dF/dt at the moment the force-drop occurs in the impedance plot. Considering phase response Conditions 8, 2 and 9, it is possible to quantify and visualize these potential masking effects.

The first effect, the base level of force, at the moment of the force drop is equal to $\Re H(j\omega)$ and is largest when $\angle H(j\omega)$ is minimal, which corresponds to Condition 8. The second effect, dF/dt at the moment of the force-drop can be derived as a function of second-order dynamics from Eq. (9) as:

$$\frac{dF}{dt}(t_{fd}) = |H(j\omega)| \cdot \omega \cdot \cos(\angle H(j\omega) + \pi/2), \qquad (16)$$

with t_{fd} being the time of the nonlinear force-drop. Both $|H(j\omega)|$ as well as ω are fixed for Conditions 8, 2 and 9 and therefore $dF/dt(t_{fd})$ can only be affected by $\angle H(j\omega)$. Furthermore, using basic trigonometry, Eq. (16) can be formulated as:

$$\frac{dF}{dt}(t_{fd}) = -|H(j\omega)| \cdot \omega \cdot \sin(\angle H(j\omega)) \qquad (17)$$

Taking $\Re H(j\omega)$ and calculating $dF/dt(t_{fd})$, the potential masking effects of second-order system phase response on friction JND (as tested in Condition 8, 2, 9) are illustrated in Fig. 20.

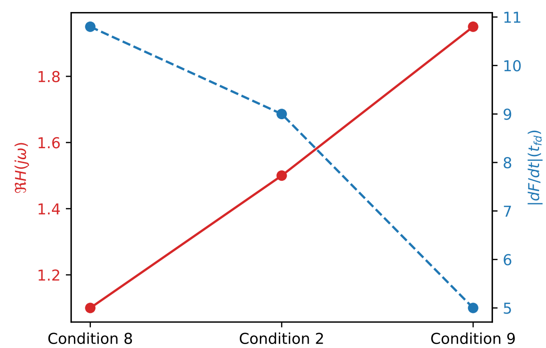

Fig. 20. Value of $\Re H(j\omega)$ and $\frac{dF}{dt}(t_{fd})$ for Conditions 8, 2 and 9 to illustrate their potential masking effects.

Fig. 21 shows the impedance plots for Conditions 8, 2 and 9 indicating both masking effects. As the figure shows, Condition 8 has the largest value for $dF/dt(t_{fd})$ while Condition 9 has the largest force at which the force drop occurs.

Considering again the detection threshold of friction being potentially influenced by $H(j\omega)$, a possible explanation for the trend of $\angle H(j\omega)$ affecting friction JND, is that $\Re H(j\omega)$ and $dF/dt(t_{fd})$ can independently increase the friction threshold when they reach certain values. Assuming an independent effect, Fig. 20 illustrates how both Condition 8 and 9 can have an increased detection threshold, caused by larger values for $\Re H(j\omega)$ or $dF/dt(t_{fd})$, respectively. Again, more research is needed to confirm these potential effects of mass-spring-damper phase response and real part on the detection threshold and therefore, indirectly, on friction JND. Further research can also aim to establish the values of $\Re H(j\omega)$ and $dF/dt(t_{fd})$, at which the detection threshold breaks down and if their effects are indeed independent.

Revisiting the main research question, formulated in the Introduction, the findings as presented in this paper show that mass-spring-damper dynamics can indeed have a masking effect on the perception of differences in friction. Furthermore, under conditions where the ratio of friction to $|H(j\omega)|$ is sufficiently large, JNDs in friction may follow Weber's law. The Weber fractions of around 20 % are close to what has been found for the tactile perception of friction in isolation [12], suggesting that these findings may be more universally applicable and not only to perceiving changes in dynamics by means of a side-stick controller. When considering the requirements of haptic feedback transparency of the CLS in flight simulator training, as set by EASA [15] and the FAA [16], the findings presented here can be combined with Fu's JND model to establish a more human-centric approach in regulating CLS transparency.

In future research, the results of this study have to be replicated, while performing more focused experiments. Furthermore, the second research question as formulated in the Introduction of how friction affects JNDs in $\Re H(j\omega)$ and

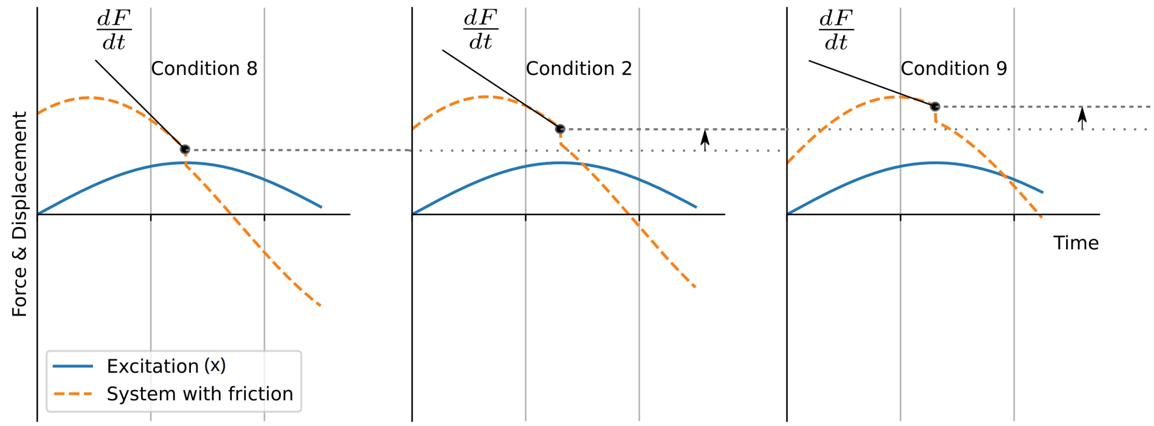

Fig. 21. Impedance plots in the time domain of Conditions 8, 2 and 9, showing the effect of second-order system phase response $\angle H(j\omega)$ on the force at which the force-drop occurs $\Re H(j\omega)$, as well as the gradient of the curve at the moment of the force-drop $dF/dt(t_{fd})$.

$\angle H(j\omega)$ should be tackled to further complement the JND model. It should be noted, however, that not knowing this effect of friction on JNDs in mass, stiffness and damping does not make the JND model less usable. It will just be more conservative as potential masking effects are not taken into account. Therefore, it is possible to start implementing human-centric design of haptic interfaces using an incomplete JND model, realizing that the current model should be considered conservative (expecting modeled JNDs to be lower than they are in reality).

A new important question that this research raises is what the detection threshold for friction is and how it behaves in the presence of second-order dynamics. This study shows that the detection threshold for friction can be influenced by mass-spring-damper dynamics, which in result affect the Weber fractions, as also illustrated in Fig. 18. To fully model JNDs in friction in the presence of second-order dynamics it might be necessary to also construct a model of friction detection thresholds, including, again, the potential effects of mass-spring-damper dynamics.

VI. Conclusion

This paper addresses the question of whether the perception of friction can be masked by mass-spring-damper dynamics, and if that is the case, how the threshold for perceiving changes in friction is affected by these linear system dynamics. An experiment was performed and results suggest that JNDs in friction follow Weber's law, also in the presence of second-order system dynamics, but only when the level of friction is sufficiently large compared to the mass-spring-damper system's impedance. Therefore, JNDs in friction are a constant proportion of reference friction, but at the limits of perception Weber's law breaks down, causing JNDs to increase. How close a specific level of friction is to the limit of perception is established from the ratio of friction to the second-order system magnitude response. Potentially, the second-order system's phase response also affects the detection threshold, independently of magnitude response, but these results are not conclusive.

References

[1] J. G. Wildenbeest, D. A. Abbink, and J. F. Schorsch, "Haptic transparency increases the generalizability of motor learning during telemanipulation," in *World Haptics Conference (WHC)*, Daejeon, South Korea, April 2013, pp. 707–712.

[2] T. B. Sheridan, "Telerobotics," *Automatica*, vol. 25, no. 4, pp. 487–507, 1989.

[3] S. Avgousti, E. Christoforou, A. Panayides, S. Voskarides, C. Novales, L. Nouaille, C. Pattichis, and P. Vieyres, "Medical telerobotic systems: Current status and future trends," *BioMedical Engineering OnLine*, vol. 15, 2016.

[4] T. Fong, J. Zumbado, N. Currie-Gregg, A. Mishkin, and D. Akin, "Space telerobotics: Unique challenges to human-robot collaboration in space," *Reviews of Human Factors and Ergonomics*, vol. 9, pp. 6–56, 2013.

[5] R. Daniel and P. McAree, "Fundamental limits of performance for force reflecting teleoperation," *The International Journal of Robotics Research*, vol. 17, no. 8, pp. 811–830, 1998.

[6] G. T. Fechner, *Elemente der Psychophysik*. Breitkopf & Härtel, 1860.

[7] L. A. Jones and I. W. Hunter, "A perceptual analysis of stiffness," *Experimental Brain Research*, vol. 79, pp. 150–156, 2004.

[8] ——, "A perceptual analysis of viscosity," *Experimental Brain Research*, vol. 94, pp. 343–351, 2004.

[9] M. Rank, T. Schauß, A. Peer, S. Hirche, and R. L. Klatzky, "Masking effects for damping jnd," in *Haptics: Perception, Devices, Mobility, and Communication*, P. Isokoski and J. Springare, Eds. Springer Berlin Heidelberg, 2012, pp. 145–150.

[10] W. Fu, M. M. van Paassen, and M. Mulder, "Human threshold model for perceiving changes in system dynamics," *IEEE Transactions on Human-Machine Systems*, vol. 50, no. 5, 2020.

[11] W. Fu, personal communication [email].

[12] D. Gueorguiev, E. Vezzoli, A. Mouraux, B. Lemaire-Semail, and J.-L. Thonnard, "The tactile perception of transient changes in friction," *Journal of The Royal Society Interface*, vol. 14, 2017.

[13] W. B. Messaoud, M.-A. Bueno, and B. Lemaire-Semail, "Relation between human perceived friction and finger friction characteristics," *Tribology International*, vol. 98, pp. 261–269, 2016. [Online]. Available: https://www.sciencedirect.com/science/article/pii/S0301679X1600116X

[14] O. Caldiran, H. Z. Tan, and C. Basdogan, "Visuo-haptic discrimination of viscoelastic materials," *IEEE Transactions on Haptics*, vol. 12, no. 4, pp. 438–450, 2019.
[15] EASA, "CS-FSTD(A): Certification specifications for aeroplane flight simulation training," Tech. Rep., 2018.
[16] FAA, "14 CFR Part 60: Flight simulation training device initial and continuing qualification and use," Tech. Rep., 2016.
[17] E. Samur, J. E. Colgate, and M. A. Peshkin, "Psychophysical evaluation of a variable friction tactile interface," in *Human Vision and Electronic Imaging XIV*, B. E. Rogowitz and T. N. Pappas, Eds., vol. 7240, International Society for Optics and Photonics. SPIE, 2009, pp. 167–173. [Online]. Available: https://doi.org/10.1117/12.817170
[18] W. Tang, R. Liu, Y. Shi, C. Hu, S. Bai, and H. Zhu, "From finger friction to brain activation: Tactile perception of the roughness of gratings," *Journal of Advanced Research*, vol. 21, pp. 129 – 139, 2020.
[19] W. Fu, M. M. van Paassen, and M. Mulder, "The influence of discrimination strategy on the jnd in human haptic perception of manipulator stiffness," in *AIAA Modeling and Simulation Technologies Conference*, no. AIAA 2017-3668, Denver, USA, June 2017.
[20] E. H. Weber, *De Pulsu, resorptione, auditu et tactu: Annotationes anatomicae et physiologicae*. CF Koehler, 1834.
[21] K. H. Norwich, "On the theory of Weber fractions," *Perception & Psychophysics*, vol. 42, pp. 286–298, 1987.
[22] W. Fu, A. Landman, M. M. van Paassen, and M. Mulder, "Modeling human difference threshold in perceiving mechanical properties from force," *IEEE Transactions on Human-Machine Systems*, vol. 48, no. 4, pp. 359–368, 2018.
[23] F. Kingdom and N. Prins, *Psychophysics: A Practical Introduction: Second Edition*. Mica Haley, 2016.

A
Staircase Method Considerations

Appendix A: Staircase Method Considerations

Staircase Implementation

The implementation of the staircase procedure is based on experiments performed by Wei Fu [1], the following principles determine the presented impedance settings:

1. The reference friction setting stays constant.
2. The compared friction setting starts out as a higher setting (for our friction JND experiments this was set at 2 times reference friction setting, whereas Wei Fu used 1.5 for the mass-spring-damping JND masking experiments).
3. The initial step-size is a fraction of the reference setting (in our case $0.4 \cdot$ reference friction).
4. The compared setting is lowered by the step-size in a correct response, while it is increased by $1.82 \cdot$ step-size (this is necessary to converge to an 80.35% correct response in a 1 down/2 up staircase according to the literature [2]) in case of an incorrect response. The staircase starts with a 1 up/1 down approach, and after the first reversal continues with 1 up/2 down.
5. Every step (regardless of stepping up, down or staying at the same level) the step-size is halved until it reaches a minimum setting ($0.05 \cdot$ reference setting) after which it is kept constant until the third reversal, at which it halves one more time (to $0.025 \cdot$ reference setting).
6. The staircase procedure lasts until the seventh reversal or after 40 steps. The last four reversals are used to calculate the Just-Noticeable Difference (JND).

This staircase procedure is based on the transformed up/down method as described by Kingdom and Prins [2] and an example of a typical full staircase is visualized in Figure 1. Starting the trial using a 1 up/1 down method until the first reversal is a way to reduce the number of trials necessary to converge and was suggested by Wetherill and Levitt [3].

Garcia-Perez [4] has run simulations performing different types of staircases and found a reliable convergence for a 1 up/2 down staircase to an 80.35% correct response when a ratio between the down and upwards step of 0.5488 was used. It should be noted that they also specify that large step-sizes should be used, anywhere between $\sigma/2$ and σ, where σ is defined as the standard deviation of the underlying psychometric function. Unfortunately, the data obtained from our staircase experiments are not sufficient to reliably estimate the psychometric functions but it should be taken into consideration in further research that step-sizes are ideally based on information or estimations of the psychometric function's parameters.

The JNDs are usually determined by averaging the difference between compared stimulus values (in this case friction settings) of all but the first reversals. In our experiment it was decided to average the values of the last four reversals, skipping the first three. This has to be the case since the staircase methods as described in [2] and [4] assume fixed step-sizes. The initial higher, rapidly decreasing step-size is used to find the region of stimulus values where to start the fixed step-size staircase method. Since JNDs can be highly variable between different subjects (as can also be seen from the Extended Results in Appendix B) it is not feasible to start with a fixed step-size since convergence would take too long, which is problematic considering fatigue and a reduced lack of focus of the test subject. Using the method of reducing the step-sizes at the start, it is possible to more quickly advance to a stimulus level close to the test subject's JND, where the step-sizes will be kept constant for the remaining steps.

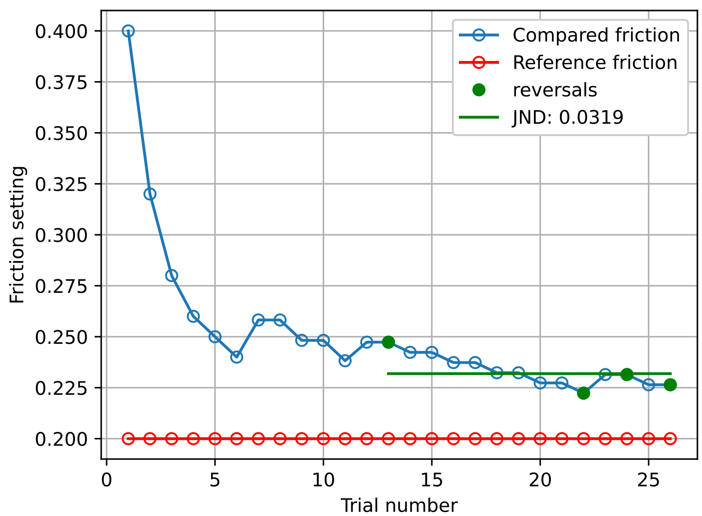

Figure 1: Example of staircase procedure with a constant step-size from the fourth reversal onward (from Participant 01 and Condition 3).

Other Approaches

Besides the 1 up/2 down staircase procedure used for our experiment several variations on this method are possible. An obvious variation is using a 1 up/1 down or a 1 up/3 down staircase procedure. If the step-size upwards is equal to the downwards step-size, 1 up/1 down procedures should converge to 50% performance, which for a two-alternative forced-choice task is equal to a performance purely based on chance. Wetherill and Levitt [3] state that the method used for our research, a 1 up/2 down procedure, converges to approximately 70.71% correct and 1 up/3 down to 79.37%.

As mentioned above, the 1 up/2 down procedure used in our experiment aims for an 80.35% correct performance JND, which is accomplished by introducing the weighted up/down method as suggested by Kaernbach [5], where the step-size down is 1.82 times lower than the step-size upwards.

From Below or From Above

In the research presented in this report it is assumed that the upper and lower JND thresholds are equal, meaning symmetric around the reference friction setting. It could be argued, however, that performing a staircase procedure from below (starting with a compared friction smaller than the reference friction and increasing the compared friction when the larger stimulus is correctly identified) results in smaller JNDs. The stimulus settings are presented to the test subject in random order and each trial should be independent to the test subject. Then, if Weber's law holds and the lower friction setting is considered the reference setting, approaching the reference friction from below (a reversed staircase procedure) would result in slightly smaller JNDs when compared to approaching the JND from above.

When the potential asymmetry of the JNDs around a stimulus baseline level is neglected, however, this leads to a conservative estimate of JNDs. With potential differences between upper and lower JNDs being very small, even though comparing them is interesting from a research perspective, the practical implications of such research will be very limited.

Hysteresis

Another way of implementing a staircase procedure is to start from a difference between the two stimulus settings which is well below the JND. From analyzing the experiment data it was found that often when test subjects get to stimulus levels well below their JND, they are not able to distinguish friction settings until well above the JND. An example of this phenomenon is given by Figure 2, where from trial 15 onward there is a clear overshoot before converging to the JND towards the end of the staircase.

What this seems to imply is that in a staircase procedure, when a test subject feels a difference between the two stimuli presented, he or she is able to continue perceiving this difference while the staircase procedure advances. However, coming from a situation where no difference is perceived, the compared stimulus intensity has to be increased well above the JND before the difference is noticed again. In other words, keeping track of a difference between two stimulus intensities is easier than first perceiving a difference.

The hysteresis effect described above could be due to the unconscious usage of specific cues in the haptic feedback. When the two stimuli can no longer be distinguished these unconsciously perceived cues may have to be reestablished, which is more difficult than just keeping track of them.

Many times during the experiment it was observed that when a test subject is presented with two different impedance settings for the same preview tracking task (as is the case for the staircase procedure), for the second impedance setting the subject would either overshoot (in case of a lower impedance) or undershoot (in case of higher impedance) the tracking task signal. This in turn helped the subject realize which of the two presented settings had a larger resistance. Interestingly, this phenomenon also shows that even if a control task is relatively unfamiliar, muscle memory can still play a role in the perception of differences, at least when the different impedance settings are presented right after one another. It is assumed that muscle memory plays a role (at least in part) when manually controlling an aircraft. Therefore, considering one of the main purposes of this research is to help tune flight simulator control loading system transparency to the resolution of human perception, the comparison of the two impedance settings depending partially on unconscious motor control, benefits the relevance of the experimental results.

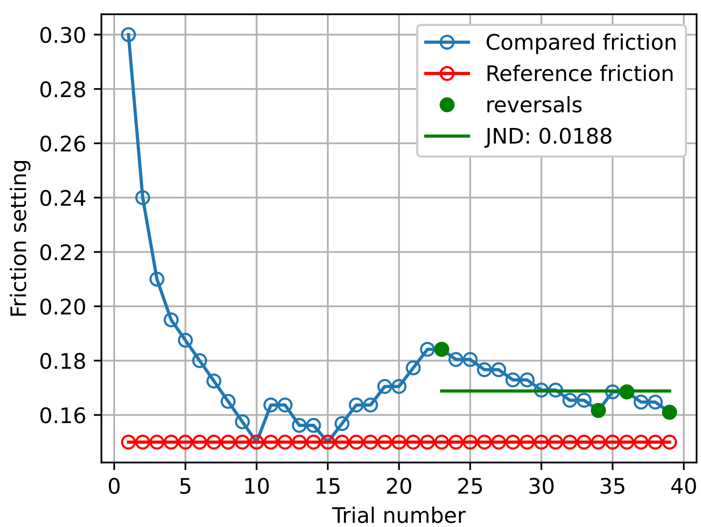

Figure 2: Illustrating the hysteresis effect. Initially, at the beginning of the staircase, the difference between both stimuli is perceived. However, from trial 15 onward, the many incorrect responses suggest that the test subject was unable to distinguish the two stimuli. The compared friction setting had to be increased to well above the JND before the test subject was able to perceive differences again. The result of this hysteresis effect is a longer trial with less than optimal convergence. (taken from Participant 08 and Condition 7)

References

[1] W. Fu, A. Landman, M. M. van Paassen, and M. Mulder, "Modeling human difference threshold in perceiving mechanical properties from force," *IEEE Transactions on Human-Machine Systems*, vol. 48, no. 4, pp. 359–368, 2018.

[2] F. Kingdom and N. Prins, *Psychophysics: A Practical Introduction: Second Edition*. Mica Haley, 2016.

[3] G. Wetherill and H. Levitt, "Sequential estimation of points on a psychometric function," *The British journal of mathematical and statistical psychology*, vol. 18, p. 1—10, May 1965. [Online]. Available: https://doi.org/10.1111/j.2044-8317.1965.tb00689.x

[4] M. A. Garcıa-Pérez, "Forced-choice staircases with fixed step sizes: asymptotic and small-sample properties," *Vision Research*, vol. 38, no. 12, pp. 1861–1881, 1998. [Online]. Available: https://www.sciencedirect.com/science/article/pii/S0042698997003404

[5] C. Kaernbach, "Simple adaptive testing with the weighted up-down method," *Perception & Psychophysics*, vol. 49, pp. 227–229, 1991.

B
Extended Results

Appendix B: Extended Results

The experiment results presented in the main paper of this report indicate that there was significant variation in Just-Noticeable Differences (JNDs) among participants. This is not just due to the differences in average JNDs between participants, because that factor has been corrected for. In this Appendix, the results of the main paper are supplemented for a better evaluation of the experiment data and to help interpret the large variance in JNDs for some experiment conditions.

Scatter Plots

The following figures show the individual JNDs for all nine participants in four scatter plots, representing the four repeated measures ANOVAs as discussed in the paper. It should be noted that the individual JNDs have been scattered to the left and right slightly, this is done to prevent them from being invisible due to overlap. It does not mean that different participants experienced different condition settings.

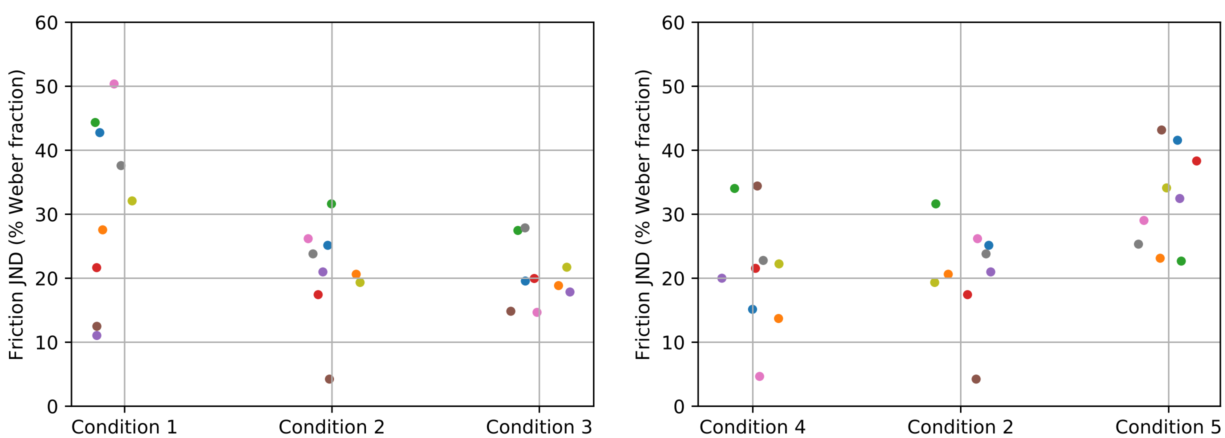

Figure 1: Scatter plots experiment Conditions 1 to 5

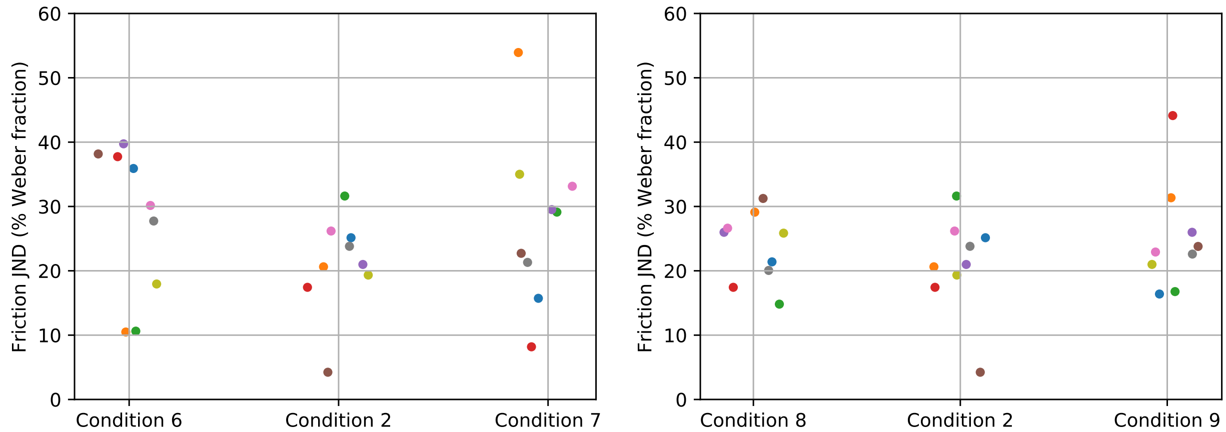

Figure 2: Scatter plots experiment Conditions 6, 2, 7 (left) and 8, 2, 9 (right)

Boxplots

The following box plots show the median, quartiles and outliers of the JND experiment data. As for the scatter plots, all four sets of conditions are plotted.

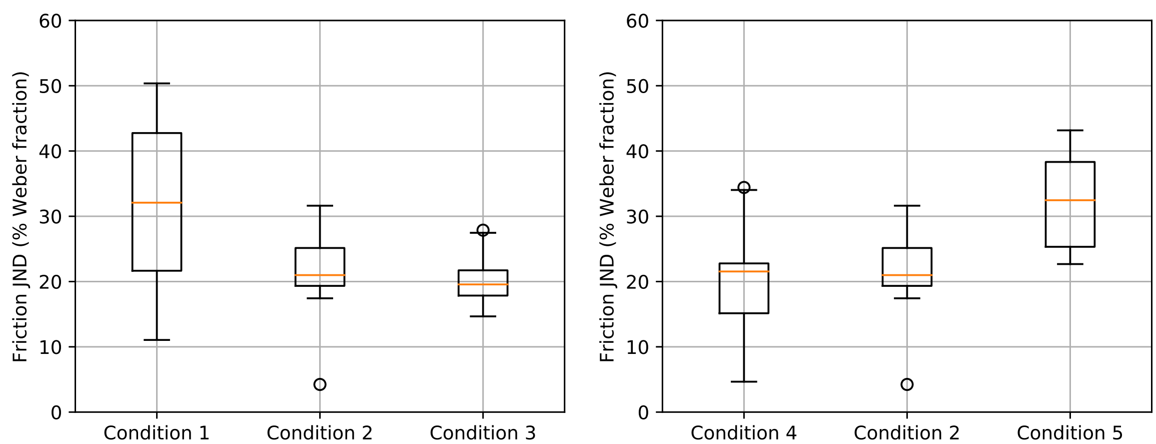

Figure 3: Boxplots experiment Conditions 1 to 5

Figure 3 shows, especially for the conditions where the spread of JNDs between participants is relatively high (conditions 1 and 4), acceptable symmetry of JNDs around the median value.

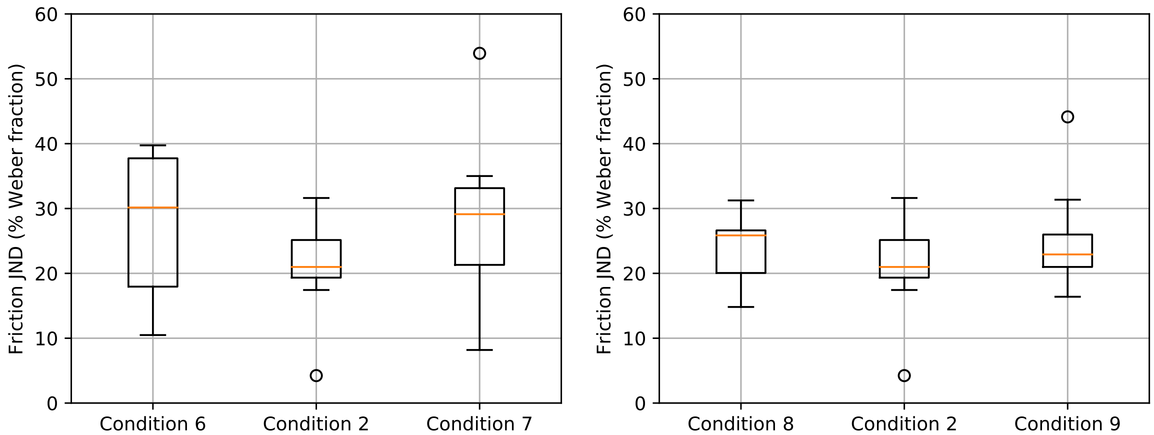

Figure 4: Boxplots experiment Conditions 6, 2, 7 (left) and 8, 2, 9 (right)

Figure 4 shows a relatively skewed distribution for conditions 6 and 7. Also the interquartile range for these conditions is relatively large, indicating that the large variance as shown in the paper is not just the result of outliers. The box plot of conditions 8, 2 and 9 also in Figure 4 show that, excluding outliers, the interquartile range between these conditions is very similar. This could indicate that the trends of a larger JND (as discussed in the paper) for $\pi/4 < \phi < \pi/4$, with ϕ indicating the phase response of the second-order system, could be due to a combination of outliers and a skewed distribution. More data are needed to draw more definitive conclusions.

C
Experiment Participant Briefing

Appendix C: Experiment Participant Briefing

1 Introduction

This document provides an overview of the experiment that is going to be conducted as part of an MSc thesis at the Technical University Delft. First, Section 2 shortly introduces the thesis and the research objective. Then, Section 3 describes the experiment, including the time planning. Finally, Section 4 discusses potential risks involved for participants and the procedure for withdrawal.

2 Research context and objective

When flying an aircraft using the flight controls, pilots experience control forces. Currently, jet aircraft always have assisted steering mechanisms, meaning the flight controls are not directly connected to the control surfaces of the aircraft, but instead, connect to a computer that translates the pilot's control inputs to moving the control surfaces. The aircraft manufacturer decides how the aircraft should feel when flying it. Additionally, for safety and comfort, the stiffness of the flight controls is usually linked to the airspeed to limit g-forces.

Ground based flight simulators are often used as an important part of a pilot's training, especially to get familiar with specific types of aircraft. It is therefore important that these flight simulators have a very similar feel to the real aircraft when it comes to the resistance to motion of the flight controls. Regulatory bodies have specified how close flight simulator control forces should match the real aircraft's control forces when using the ground based simulator for pilot training. However, currently, these requirements do not take the precision of human perception into account and it may therefore be possible to relax requirements without a noticeable drop in fidelity.

This research focuses on a specific part of the resistance of flight control columns, namely friction. Currently, it is not clear to what extend pilots are able to distinguish different levels of friction when there are other forces present (like stiffness or damping). The minimum perceivable difference in forces is called the Just Noticeable Difference (JND). The experiments for this research are focused on finding a relationship between these JNDs in friction and other flight control force parameters (for example stiffness or damping forces). The main objective of this research is then to construct a first model of JNDs in friction in flight controls. This understanding of JNDs in friction will add to the body of knowledge necessary to optimize requirements of flight simulator control forces fidelity.

3 The experiment

For this experiment, nine participants will carry out multiple preview tracking tasks. The task is visualized in Figure 1b, where the participant has to follow the sinusoidal motion with the joystick by making the circle move together with the cross as much as possible. This will be practiced a few times before starting the actual experiment. For each participant there will be nine conditions of different joystick resistance settings and for each condition there will be anywhere from 20 to 40 trials. During each of these trials the participant performs the tracking task two times for approximately six seconds with minimal time in between. Then the participant will give feedback to the researcher for which of the two instances the stick was harder to move (so the participant has the option to choose between the first or the second instance). This is repeated for 20 to 40 trials until the JND for that specific participant and condition is established. For nine conditions this takes approximately 1 hour and 20 minutes.

(a) Joystick and task display

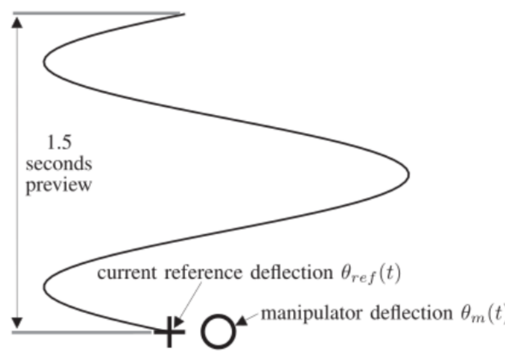

(b) Preview tracking task on the display

Figure 1: Experimental setup, *Reprinted from W. Fu, A. Landman, M. M. van Paassen, and M. Mulder, "Modeling human difference threshold in perceiving mechanical properties from force," IEEE Transactions on Human-Machine Systems, vol. 48, no. 4, pp. 359–368, 2018.*

Because the participant has to both follow a tracking task while also paying attention to the resistance of the flight stick, which can be tricky in the beginning, it is important to practice this before starting the actual experiment. During this training the participant has to reach a certain accuracy for the control task, as well as give consistent feedback on which instance of six seconds the stick felt heavier to move. Consistency in this case means that during the training the participant will perform a condition for which the JND has to converge showing the participant is consistent in their feedback on flight stick resistance. Because of the repetitive nature of the test also several breaks will be included to make sure participants can stay focused on the task and will not get bored or distracted. The complete time planning for the experiment is given in Figure 2.

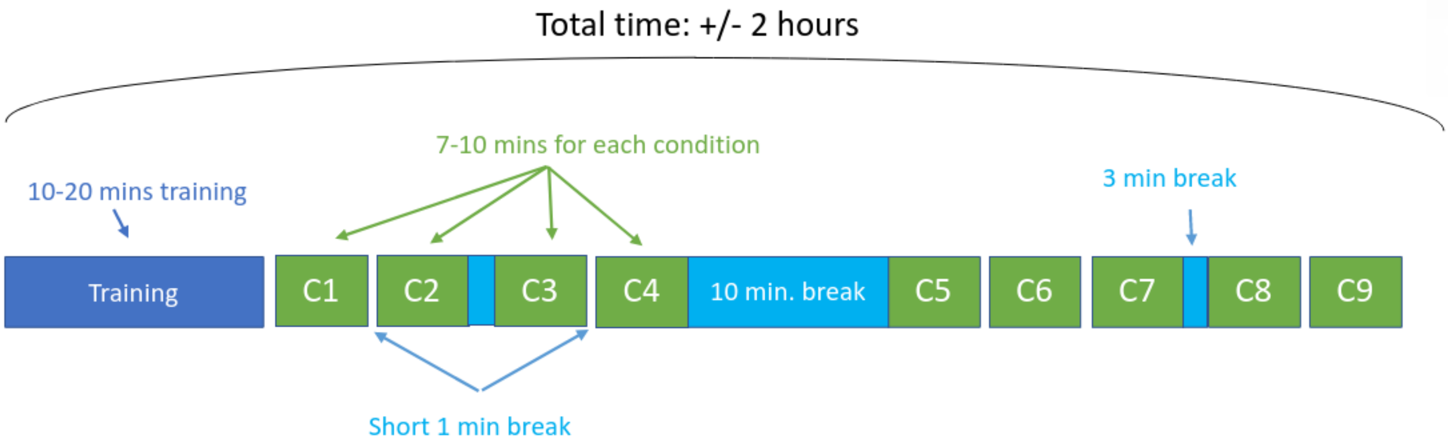

Figure 2: Time planning of the experiment

4 Risks and withdrawal

As can be imagined from the experiment description, there is minimal risk involved in participating. In storing the JND measurement data, participant numbers will be used in labelling so there is no way to retrace it to a specific participant. The only personal information that will be collected is the name and signature on the consent form, which will be digitally stored on a storage drive at the TU Delft, accessible only by the project supervisor Dr. ir. René van Paassen (up to 10 years after project completion). Aside from the privacy risks, there are virtually no risks involved considering the psychological and physical well-being of the participants. The required control forces are low so muscle soreness afterwards is unlikely, leaving boredom as the only risk, which is dealt with by including multiple breaks. In any case, a participant can withdraw from the study during any phase of the experiment without an explanation.

D

Preliminary Report

JND in friction

Extending a model of Just Noticeable Differences in second order dynamics to the non-linear case

R. Veldhuis

Appendix D: Preliminary Report (Already Graded)

TU Delft

JND in friction

Extending a model of Just Noticeable Differences in second order dynamics to the non-linear case

by

R. Veldhuis

Student number:	4138570	
Project duration:	October, 2020 – currently ongoing	
Supervisors:	Prof. dr. ir. M. Mulder,	TU Delft, Aerospace Engineering, C&S
	Dr. ir. M. M. van Paassen,	TU Delft, Aerospace Engineering, C&S

TU Delft

Contents

1 Introduction

Ever since the Digital Revolution, starting in the second half of the 20th century, the interaction of humans with the environment has changed significantly. Specifically in the domain of human-machine systems, perception of the environment often occurs solely through digital interfaces. The obvious benefits are plentiful. Not only can the visual, aural or haptic feedback be adjusted and extended in ways that seem unthinkable when using only analog systems, but it can also, more easily, take place at a physically different location. This allows for teleoperation, as described by Sheridan [1], applied to different disciplines, from medicine [2] to space exploration [3]. Also, simulating reality has become more and more accurate. In aviation, this has opened the door to pilot training in ground based simulators. The flight simulators that can be used for this purpose follow strict specifications as formulated by, among others, the European Union Aviation Safety Agency (EASA) [4] or the Federal Aviation Administration (FAA) [5]. Requirements on fidelity are given for the simulated aircraft's flight model but also for visual, aural and haptic cues. This report focuses on these haptic cues and more specifically the human perception of haptic feedback.

1.1. Background

Traditionally, flight control forces in aircraft were determined by the aerodynamic forces on the control surfaces and their mechanical design. With this so called reversible control system there is a direct link between the aircraft state and the haptic feedback on the flight controls. For most general aviation aircraft, this direct link has remained. However, modern airliners, due to required forces being much higher, have all adopted irreversible controls which may reduce the richness of the haptic feedback to the pilot. This haptic feedback gives the pilot an indication of the state of the aircraft and can therefore aid pilots in their task of controlling the aircraft. Some properties of the reversible control systems, like higher stiffness at higher speeds, have been implemented into irreversible flight controls to account for the loss of haptic feedback. In flight simulation, a control loading system (CLS) is used to simulate the control forces present during actual flight.

1.1.1. Control Loading Systems

Flight simulators as training devices are an effective tool to practice procedures, especially for events that would be dangerous in real life. Furthermore, the usage of ground based simulators can significantly reduce flight training costs. To ensure training in the flight simulator carries over to better performance in the real aircraft it is important to define the simulator fidelity. Different aspects of training require different levels of fidelity. It is important to realize higher levels of fidelity are not always required for optimal training. This "disconnect" between fidelity and validity is important to understand since a lower fidelity simulation may complement the higher fidelity simulation training such that it makes the pilots more resilient to unanticipated escalating events [6]. However, when training manual flight, the feel of the simulator's flight controls, is essential for the development of the motor skills necessary for controlling a specific aircraft.

Requirements have been developed by EASA and the FAA, which define maximum differences in flight stick dynamics between the real aircraft and the flight simulator under different flight conditions [4],

[5]. These requirements on haptic display transparency beg the question of how they relate to human force perception. That is, will humans actually perceive the differences between different CLS settings, or levels of CLS transparency.

1.1.2. Force Perception and Just Noticeable Differences

Force perception and the ability to detect differences in force stimuli is described in the field of Psychophysics, which is defined as the subfield of Psychology where the interaction between physical stimuli and the sensory system is studied [7]. Fechner formulated Weber's law, which states that a minimal detectable change in a stimulus is directly proportional to the intensity of the initial stimulus [8]. This so called just noticeable difference (JND) can be defined for different types of stimuli, e.g., sound, vision, touch, taste and smell.

1.1.3. A Unified Just Noticeable Difference Model

The relationship between human perception and the EASA/FAA definitions of required accuracy for the CLS is not fully understood. Translating JNDs in flight stick impedance to criteria for haptic feedback transparency is difficult because they depend on multiple properties of the system.

In recent years, research by Fu [9] has given some fundamental insights into JNDs in second order (mass-spring-damper) linear systems. Several experiments were performed using a hydraulically powered admittance display in the form of a flight stick. The JNDs in mass, stiffness and damping were found to be proportional to the magnitude response of the system resulting in a model of JNDs in second order systems. Therefore, JNDs in stiffness, mass and damping depend on the excitation frequency of the system, as well as the real (stiffness and mass) and imaginary (damping) part of its response.

The significance of this finding is that it shows the masking effect of damping on mass and stiffness JND and vice versa. With a good understanding of the JND in second order control force dynamics, it is possible to optimize the transparency of the CLS of flight simulators and training devices. If there is a disconnect between current CLS requirements on transparency and human perception, then it may be possible to enhance the EASA and FAA requirements based on knowledge about the perception of stick dynamics and the relevant JNDs. This could then lead to lower cost and complexity of the CLS.

The current understanding of JNDs and control forces, however, is not extensive enough for such conclusions. The model of Fu [9] only considers linear systems and in reality control forces also include non-linear effects. Therefore this research is aimed at contributing to the development of a more encompassing JND model, for the purpose of this report this hypothetical JND model will be named the Unified JND Model.

A very pronounced nonlinear factor when it comes to control force dynamics is friction. The effect of friction on the stick dynamics obviously depends heavily on the aircraft type. For some aircraft though, like the Boeing 737 max/NG, the control column friction can be very substantial at around 3-5 kg [10], which is around 10% of the control column's spring force at maximum excitation. Therefore, understanding friction is important for developing this Unified JND Model.

1.2. Research Objectives and Questions

The main objective of this research is defined as follows:

> ***"To extend the current understanding of just-noticeable differences in second order stick dynamics to the nonlinear case by introducing friction."***

It will follow up on the work of Fu [9] by taking his JND model as a starting point. Friction is one of the main nonlinear effects that is lacking in the current model, as friction has a relatively large contribution to the total flight stick impedance. Therefore, adding friction to second order stick dynamics and re-evaluating thresholds for perceiving changes in dynamics (JNDs) is a logical extention of the current research and the model formulated by Fu.

It is chosen, for the purpose of this thesis, to initially investigate the friction JND in the presence of second order dynamics as opposed to researching the potential masking effect of friction on mass, spring and damping JNDs. Formulated as research questions both suggestions are given below:

1. "What is the friction JND in the presence of second order dynamics?"

2. "How does friction, when added to a second order system, affect stiffness, mass and damping JND?"

Both questions need to be solved in order to construct a Unified JND Model, however, combining them into a single research question would convolute this thesis unnecessarily. Furthermore, it could be argued that the first question of how well changes in friction are perceived is a more fundamental one and should thus be studied first. From answering this first question an hypothesis can be formulated on what the Unified JND Model, which includes a friction component, looks like. Research question 2 can then be considered to test this model, but this will be beyond the scope of the current research.

There are several sub questions that should be addressed in order to answer research question 1. Initially, one could think that friction JND follows Weber's law and that the presence of a mass-spring-damper system does not have any masking effect on the friction JND, meaning the friction JND would depend on the reference level of friction and not the mass-spring-damper system its added to. Therefore, the first subquestion is:

1.1 "Does friction JND merely depend on reference friction when its added to a mass-spring-damper system?"

If this is not the case, then the mass-spring-damper system does have a masking effect, resulting in a higher friction JND. The next sub-question focuses on understanding this relationship between the mass-spring-damper system parameters and friction JND.

1.2 "What is the relationship between the mass-spring-damper system parameters and friction JND?"

To answer these research questions, the problem will first be studied using a model-based analysis with calculations of mechanical impedance of the mass-spring-damper system with added friction. Based on this analysis and previous research, hypotheses can be formulated that will ultimately be tested in an experiment. For this experiment a sinusoidal tracking task is chosen as it is necessary for a frequency domain analysis of the problem, and thus for building upon Fu's JND model [9].

In his thesis, Fu [9] demonstrates how the parameters of mass, spring and damping can be split up into an in-phase (real-part) and out of phase (imaginary part) response of the second order dynamics, with mass and spring properties relating to the real part of the system and damping relating to the imaginary part. Grouping the system parameters like this leaves for two potential masking effects, in more detail, the above research question 1.2 can then be divided into more specific subquestions:

1.2.a "Given a second order system with added friction, how does changing the real part (mass/spring) of this system affect the JND in friction?"

1.2.b "Given a second order system with added friction, how does changing the imaginary part (damper) of this system affect the JND in friction?"

1.3. Report Outline

This report is structured as follows. Chapters 2 and 3 will cover the first part of this report and discuss a literature study. Then Chapters 4 and 5 will discuss a preliminary analysis of the research question which is considered the second part of the report. In Chapter 2, the literature study starts with a brief overview of force perception and thresholds for perceiving changes in second order system dynamics and friction. Chapter 3 will then go into more detail regarding second order systems and the research into developing a unified JND model. Then, after discussing the literature, in Chapter 4, a first analytical analysis of the perception of friction will be presented and reflected upon. Following the analytical analysis, hypotheses are substantiated in the same chapter. Chapter 5 then describes the experiment that will be conducted to answer the research question formulated in the introduction.

2
Force Perception

In this chapter a very brief historical overview is given of the research into the sense of touch. It is narrowed to the interest of this thesis which is the perception of force differences and more specifically the perception of friction. Towards the end of this chapter the EASA and FAA requirements on transparency of the control loading system (CLS) will be discussed.

2.1. Weber's Law

Early in the 19th century, German anatomist and physiologist Ernst H. Weber defined the concept of just-noticeable difference as the smallest perceivable change in stimulus [11]. Mathematically this definition is described by Weber's Law [12]:

$$\frac{\Delta I}{I} = k \tag{2.1}$$

Here, I is the intensity of an initial stimulus, ΔI is a change in stimulus that will be just noticeable and k is a constant called the Weber fraction. Equation 2.1 states that when exposed to an initial stimulus I, the just-noticeable difference stimulus ΔI will be proportional to that initial stimulus. Whereas Weber gathered his data during weightlifting experiments, Gustav T. Fechner, a student of Weber, later confirmed its wider applicability to other senses like vision and hearing. In the past centuries the law has been shown to hold over a wide range of sensing and only breaks down at the upper (limit of damage to sensory organs) and lower limit of sensation, which is not the region of interest of this thesis. [11]

2.2. Psychophysics

Later in the 19th century, Gustav T. Fechner, published "*Elemente der Psychophysik*" [8], in which he mathematically elaborated upon Weber's law. To find a relationship between the physical world and the psychical, Fechner had to establish measurements of mental processes [13] which is particularly challenging because of their subjective nature. His solution to this problem was to measure relative increase in mental intensity as a function of the required physical intensity [8]. He realized Weber's definition of just noticeable difference could be used as a subjective unit of measurement.

Elaborating upon Weber's law he formulated the Fechner law, as given by Equation 2.2, relating perceived stimulus intensity to measured physical stimulus intensity [14]:

$$P = k \ \ log I \tag{2.2}$$

Here, P is the perceived stimulus intensity and I is the physical stimulus intensity. The constant k can be determined for different senses within the range for which Weber's law holds. To be able to use the JND as a unit of measurement it was important for Fechner to realize accurate measurements of these JNDs. Three different methods for determining them were studied by Fechner. A brief explanation of each is given below [12].

Method of limits: Two stimuli are presented to the subject. One stays constant, while the experimenter slowly reduces the intensity of the other stimulus from above the detection threshold to below. The range over which these two stimuli are perceived equal determines the JND.

Method of average error: Similar to the above, two stimuli are presented. One stays constant, while the other is (in this case by the subject) adjusted until the signals are perceived equal. The probable error of the adjustment can then be used to determine the JND.

Method of constant stimuli: In this case multiple stimuli are presented that have to be compared to a baseline stimulus. The subject is asked which of the presented stimuli is greater than the baseline stimulus. The probability of a correct answer is a smooth function of the difference between the baseline stimulus and the stimulus to be judged. The function is called the psychometric function.

Many years later, more efficient variations of these basic methods have been established. An example is the truncated staircase procedure, which is a relatively simple extension of the method of limits. Starting from a difference between two stimuli which is far above the JND, the stimulus with the largest magnitude is lowered with fixed steps towards the baseline stimulus, which is held constant. Test subjects have to determine which of the two stimuli has the highest magnitude and when correct the adjustable stimulus will be lowered towards the baseline stimulus. If the subjects answer incorrectly then the direction changes and the adjustable stimulus' magnitude will be increased. These direction changes will settle around an average that can then be used as a JND estimate. [15]

2.3. Perception of Second order Dynamics

Weber's notion of just noticeable differences was based on weight lifting experiments. But later towards the end of the previous century, his law was being applied to more complex examples of perception. For instance, Jones et al. studied the perception of both stiffness [16] and viscosity [17] using Weber's law and determined their respective Weber fractions in elbow flexion using two electromagnetic motors. With the wrist of one arm attached to the "reference" motor, the subjects adjusted the other motor (coupled to the other arm's wrist) until the stiffness (or viscosity for the second study) was perceived equal.

Jones et al. found, using this method which is similar to the "Method of Average Error" described earlier, that for both stiffness and viscosity the Weber fractions were constant over a large range (and Weber's law also holds for stiffness and viscosity perception). For low values of stiffness and viscosity, however, the Weber fractions were found to be significantly higher. Meaning, at stimulus intensities closer to the lower limit of sensation, JNDs in stiffness and viscosity will be larger. For the stiffness experiments the resulting Weber fractions can be seen in Figure 2.1. The viscosity JNDs followed a similar pattern as seen in Figure 2.2.

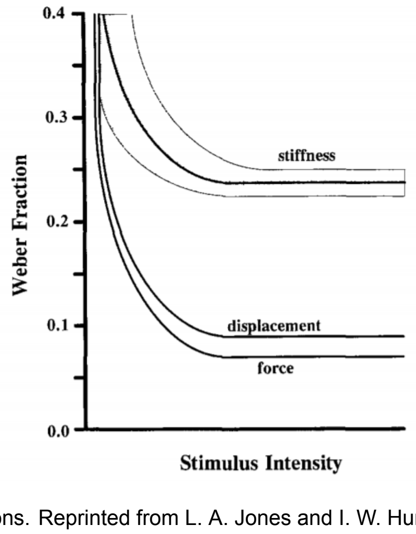

Figure 2.1: Stiffness Weber Fractions. Reprinted from L. A. Jones and I. W. Hunter, "A perceptual analysis of stiffness," Experimental Brain Research, vol. 79, pp. 150–156, 1990.

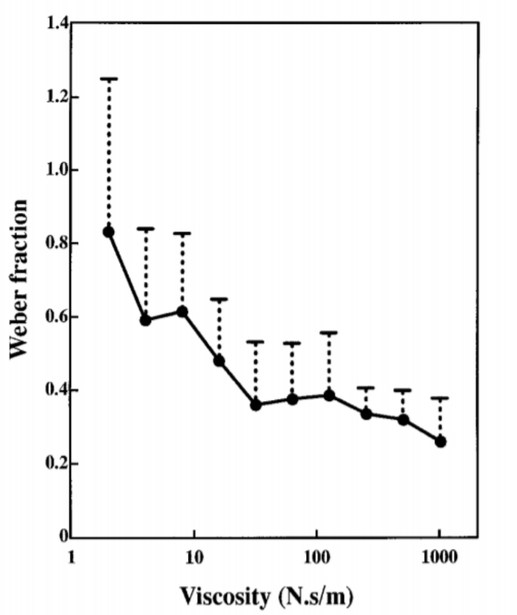

Figure 2.2: Viscosity Weber Fractions. Reprinted from L. A. Jones and I. W. Hunter, “A perceptual analysis of viscosity,” Experimental Brain Research, vol. 94, pp. 343–351, 1993.

Since participating subjects were blindfolded during the experiment they had to rely on proprioceptive sensing of angle and velocity when feeling the resistance to rotation. Only the combined information of force and motion would be helpful in order to match stiffnesses and viscosities. Furthermore, subjects were not given any instruction on which cues to use in the identification of the motor impedance. Most subjects, however, reported the use of similar strategies, they did not use the full range of motion but made small oscillatory movements.

Another observation Jones makes in his studies is the considerable intra-individual variability in the judgement of both stiffness and viscosity. This is also a possible explanation for why subjective measurement scales of muscle tone (as used for judging spasticity, dystonia and Parkinson’s disease), have always had a relatively poor inter-rater reliability [18], [19]. So even though subjects were able to distinguish different levels of stiffness and viscosity quite accurately over a wide range of perception (for elbow flexion the Weber fraction’s were estimated around 0.23 and 0.34 for stiffness and viscosity, respectively), the intra-individual variability in judging is relatively high. According to Jones, it is unknown whether this variability can be reduced by training.

2.4. Perception of Friction

The literature on the perception of friction is not very extensive and when available it is mostly related to tactile perception for the purpose of touch displays [20]–[22]. JNDs in friction might be different when considering tactile perception of the fingers compared to larger forces on a limb. For the latter, proprioception heavily depends on the muscle spindles and Golgi-tendon organs but for feeling the friction between the skin and a tactile surface mechanoreceptors might play a more important role [23].

Nevertheless, Weber’s law has been shown to (roughly and with some limitations) hold for a variety of different senses and circumstances [8] as long as extremes in sensation are not considered. That is also what Samur et al. [21] found. When studying the JND in friction by sliding a finger across a surface with an adjustable friction coefficient, they found a constant Weber fraction over the entire range of measurements. Figure 2.3 shows the experimental setup used. The friction coefficient was varied by vibrating the glass at ultrasonic frequency which creates an air pocket between the finger and the glass. This air pocket influences friction levels.

Gueorguiev et al. [22] performed a similar experiment but in this case the finger was enclosed and did not make direct contact with the tactile surface for which friction parameters were varied. They also found a constant Weber fraction for friction JND.

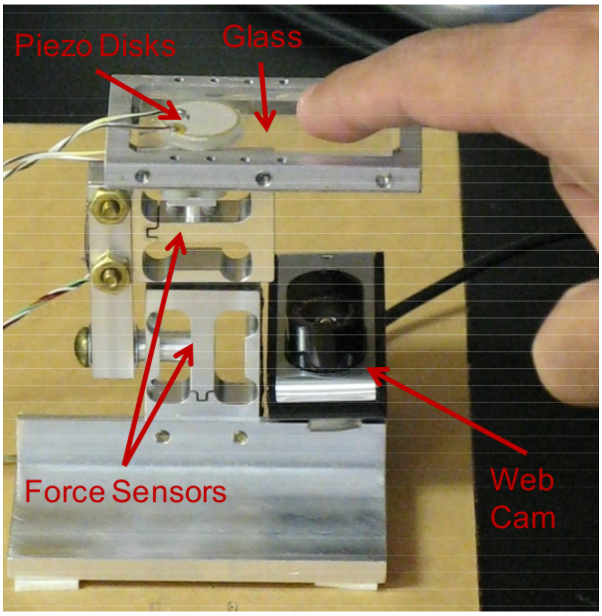

Figure 2.3: Experimental setup Samur et al. Reprinted from E. Samur, J. Colgate, M. Peshkin, B. Rogowitz, and T. Pappas, “Psychophysical evaluation of a variable friction tactile interface,” Jan. 2009.

2.5. Control Loading Systems

The CLS of a flight simulator or flight training device is used to simulate the dynamics of the control forces present when flying the real aircraft. The accuracy of this system is critical for training pilots as it allows them to develop ’muscle memory’, creating an internal model of the dynamics and associated tactile characteristics [24]. This internal model can be developed for both common flying scenarios, as well as for situations that would be very rare or dangerous when performed in a real aircraft. Traditionally, the haptic feedback of the controls in flight simulators are hydraulically controlled, but electrical systems have been the standard for the last few decades [25].

2.5.1. Control Forces

Control forces can be modelled using second order dynamics while adding friction as non-linearity. In Figure 2.4, a slow cycle of a typical control device is shown. The figure shows the control column’s impedance to slowly varying the angle over the full range of motion. Since the movement occurs at a very slow but constant speed, the dynamics reduce to that of a spring (or two springs of different stiffnesses) with added friction (both static and dynamic). Also a breakout force can be distinguished, which is the force necessary to move the stick out of the center position.

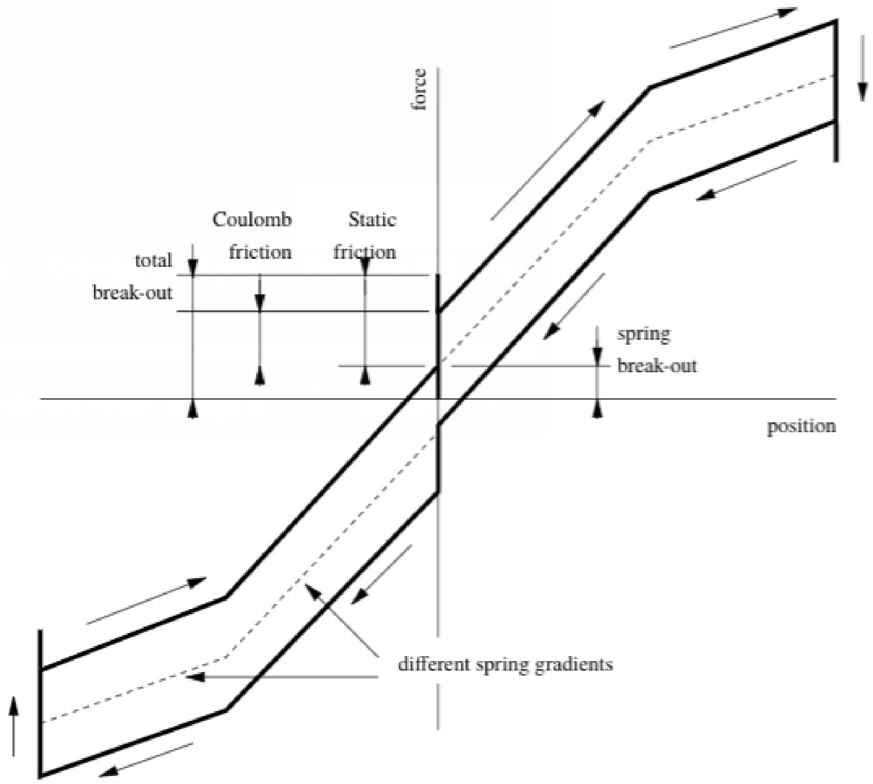

(a) Illustration of break-out force, static friction and Coulomb friction force, in a hypothetical slow cycling of a control device.

Figure 2.4: Control Forces. Reprinted from M. M. van Paasen, Ae4322 reference: Control loading systems, 2018.

2.5.2. FAA & EASA Requirements

As discussed before, the accuracy of the control loading system is critical for training manual flight in a flight simulator. Both EASA (CS-FSTD(A) [4]) and the FAA (14 CFR Part 60 [5]) have defined requirements for the control loading systems of flight training devices or simulators.

Requirements on the control forces accuracy are given for different flight scenarios under different aircraft configurations. These are often given as a percentage of deviation between the control forces caused by the CLS and the control forces as measured in the real aircraft. The EASA regulations also consider cycles of different speeds throughout the full range of motion of the control columns. Three cycles are distuingished. A static test where a full sweep of the controls (moving the controls over their entire range of movement) is realized in 100 seconds. At this speed the resistance of the control column will be determined mostly by friction and stifness. To test the CLS impedance, dynamic testing is done. For these tests the same sweep of the controls is done at both 10 seconds and 4 seconds for the entire movement. Tolerances for these sweeps are defined in tables [4].

Furthermore there is the free response test of the CLS. Moving the control column to its extreme position and measuring the free response dynamics which can be either underdamped or overdamped (and critically damped). Figure 2.5 shows the parameters of the free response (underdamped) that are considered when validating the CLS. In Figure 2.6 the same graph is shown for the overdamped or critically damped response.

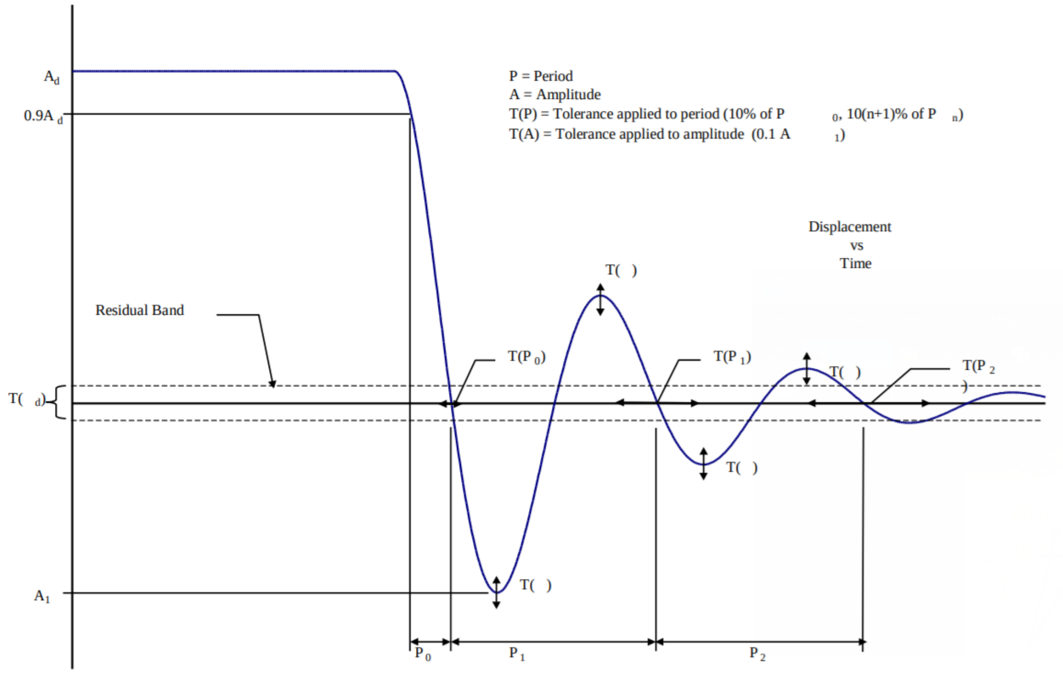

Figure 2.5: Tolerances of underdamped free response. Reprinted from EASA, “CSFSTD(A): Certification specifications for aeroplane flight simulation training,” Tech. Rep., May 2018.

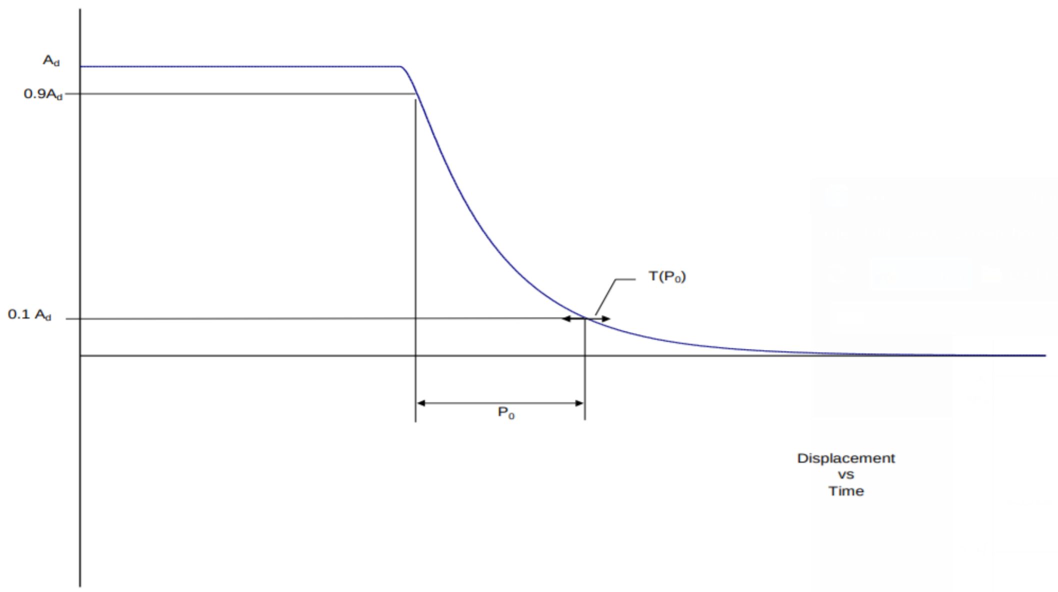

Figure 2.6: Tolerances of over-damped or critically-damped free response. Reprinted from EASA, “CSFSTD(A): Certification specifications for aeroplane flight simulation training,” Tech. Rep., May 2018.

It is obvious that relating these validation tests to human perception of control force dynamics is not straightforward. Finding the friction, stiffness, damping and mass parameters of the second order system corresponding to the control force dynamics (and thus tolerances in these second order dynamics parameters) is possible. However, the way these tolerances are defined indicates that they are not based on the human perception resolution. To optimize CLS design, a more human-centric approach is necessary. Finetuning the tolerances as given in Figure 2.5 and 2.6 to a model of human JNDs could potentially reduce cost and complexity of the CLS.

3
A Unified JND model

The relationship between human perception and the definitions of required CLS accuracy by EASA or the FAA is not fully understood. Fu [9] studied this problem and formulated a model of JNDs in a second order system, as a function of the real and imaginary part of the system response as well as the excitation frequency. What is novel about this research is that stiffness, damping and mass were not looked at in isolation but also their interaction was studied [26]. From previous research it was found that damping JND is affected by increased stiffness or mass [27], showing they can act as a masking stimulus. In this chapter, Fu's JND model will be discussed, as well as other research groups studying the perception of changes in system dynamics.

3.1. JND Model Fu

Fu et al. [26] studied the perception of changes in system dynamics using a mass-spring-damper system (a second order system). The general equation that describes the free response of a second order system is given as:

$$m\ddot{x}(t) + b\dot{x}(t) + kx(t) = F(t) \tag{3.1}$$

Here, m is the mass and b and k the damping and the stiffness coefficient, respectively. The displacement x and force F are given as a function of time. When Laplace transforming Equation 3.1 it is possible to derive a transfer function describing force per displacement:

$$ms^2X(s) + bsX(s) + kX(s) = F(s) \tag{3.2}$$

Looking only at the steady-state response the Laplace variable s becomes jω:

$$k - m\omega^2 + b\omega j = \frac{F(j\omega)}{X(j\omega)} = H(j\omega) \tag{3.3}$$

From Equation 3.3, the real $(k - m\omega^2)$ and imaginary $(b\omega)$ part of the transfer function $H(j\omega)$ can be distinguished. The real part corresponds to the stiffness and mass contribution to the mechanical impedance in the frequency domain and the damping is represented by the imaginary part. Figure 3.1 shows this force displacement relationship, where the system is sinusoidally excited, in time.

From Figure 3.1 it can be seen that the real part ($\Re H(j\omega)$) of $H(j\omega)$ shows an in-phase response and the imaginary part ($\Im H(j\omega)$) is $90\,\deg$ out of phase. Figure 3.2 shows the response of Figure 3.1 in the complex plane.

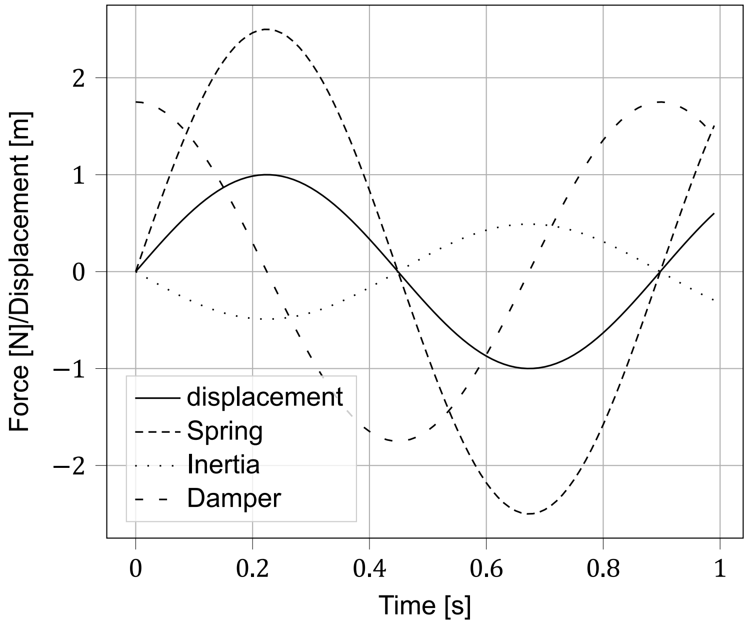

Figure 3.1: Force-Displacement (steady state) graph for typical second order system ($k = 2.5$, $b = 0.25$, $m = 0.1$)

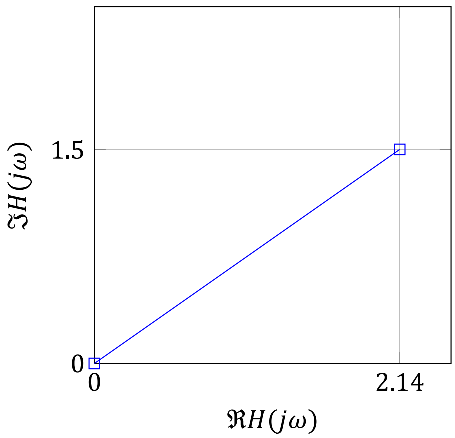

Figure 3.2: Complex-plane representation of $H(j\omega)$ ($k = 2.5$, $b = 0.25$, $m = 0.1$) as seen in Figure 3.1

Fu et al. performed multiple experiments where the mechanical impedance of the system was varied both by changing the real part (stiffness and mass) of its frequency response as well as the imaginary part (damping). In different system configurations (varying $H(j\omega)$) the JND (both in the real part $\Delta\Re H(j\omega)$ and imaginary part $\Delta\Im H(j\omega)$) was determined. The experiments were performed using an hydraulically controlled admittance display in the form of a side stick. Subjects were asked to perform a sinusoidal movement by using the side stick manipulator in a preview tracking task. Figure 3.3 shows this experimental setup. At every setting of $H(j\omega)$ subjects had to perform the same sinusoidal tracking task for two settings. A reference $H(j\omega)$ as well as an incremented $H(j\omega) + \Delta\Re H(j\omega)$ or $\Delta\Im H(j\omega)$. Then a staircase procedure as described in [28] was used to determine JNDs.

By analyzing the JND results from the experiments, Fu et al. found an expression for a unified JND model in second order system dynamics. The model can be seen as an extension of Weber's law and is given by:

$$\left|\frac{\Delta\Re H(j\omega)_{jnd}}{H(j\omega)}\right| \approx \left|\frac{\Delta\Im H(j\omega)_{jnd}}{H(j\omega)}\right| = constant \tag{3.4}$$

This equation states that the JND in stiffness or mass, as well as in damping, is proportional to the magnitude of $H(j\omega)$ (the magnitude response of the system). This means the JNDs in stiffness, mass

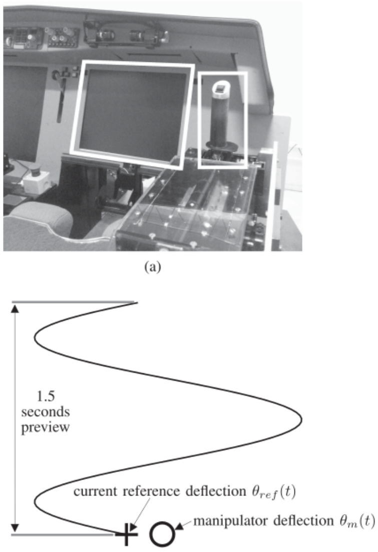

Figure 3.3: Experimental setup Fu et al., Reprinted from W. Fu, A. Landman, M. M. van Paassen, and M. Mulder, "Modeling human difference threshold in perceiving mechanical properties from force," Aug. 2018.

or damping can be expressed as a function of the system's initial stiffness, mass, damping and also the frequency of the system. Nevertheless, Fu et al. state that it is not clear yet what the JND would be when changing both $\Re H(j\omega)$ and $\Im H(j\omega)$ simultaneously. This would mean changing the system dynamics in the radial direction in the complex plane, and thus performing a different experiment.

3.2. Discrimination strategies

Fu also discussed an experiment in his thesis [9] studying the different possible discrimination strategies in perceiving differences in stiffness. The same admittance display was used as in the experiments described in the previous section. Three conditions where considered for which the stiffness JND was determined. A force condition where subjects performed a task with constant displacement, so because of a change in stiffness the force would change and force perception determined the JND. A displacement condition where subjects would be guided to excite the system with the same force and therefore different displacements. Finally, a third condition would leave the subjects with both force and displacement feedback allowing them to freely move the manipulator any way they deemed fit. It was found that the force condition resulted in the lowest JND. This means the perception of small changes in system dynamics is most likely largely based on changes in force and the perception of displacement may not be very accurate. This result seems to be consistent with the JND model as given by Equation 3.4, since the system's magnitude response corresponds to the highest force perceived. The JND is then proportional to this maximum force.

3.3. Other Research

Another research group that has been studying the perception of damping and stiffness (they use the terms viscosity and elasticity) is from Koc University, Istanbul. Caldiran et al. [29] studied the perception of a visco-elastic surface using the experimental setup shown in Figure 3.4. Similar to Fu's experiments [26], a combination of haptic as well as visual cues were available to the experiment's participants. In the frequency domain, firmness and bounciness were defined as the magnitude and phase response, respectively. Then two experiments were performed studying both the bounciness and firmness JNDs. This can be expressed as moving the system's response in the imaginary plane in either the radial (firmness) direction or changing the phase (bounciness) as shown in Figure 3.5. Therefore, when comparing it to Fu's approach, it is a description of JNDs in the imaginary plane in polar coordinates. Where Fu was studying the JND in $\Re H(j\omega)$ and $\Im H(j\omega)$ which is more of a Cartesian approach to the imaginary plane.

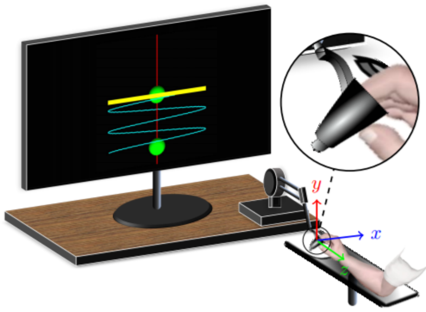

Figure 3.4: Experimental setup Caldiran et al., visual cues were rendered on the LCD display where the participants moved the yellow bar between the green dots. Haptic cues were rendered using a Phantom Premium 1.0 device. Reprinted from O. Caldiran, H. Tan, and C. Basdogan, "An investigation of haptic perception of viscoelastic materials in the frequency domain," Apr. 2018.

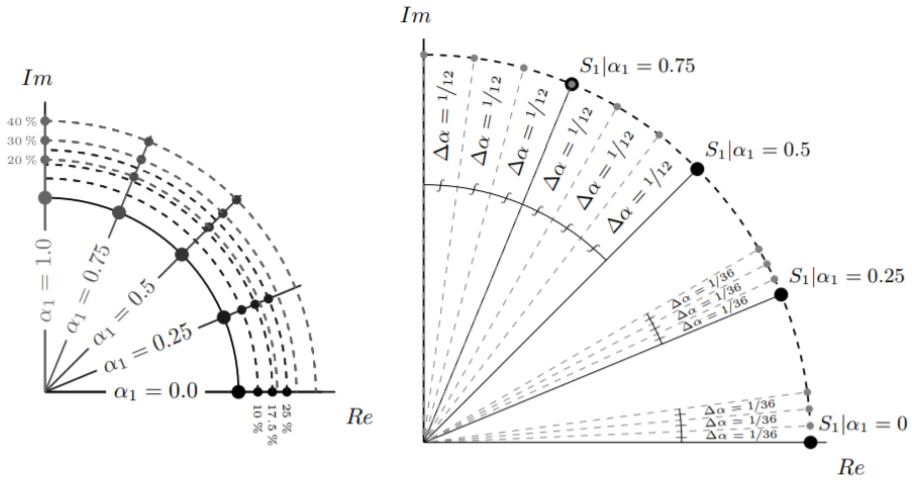

Figure 3.5: Experiment conditions Caldiran et al. in the imaginary plane for the bounciness experiment on the right and the firmness experiment on the left. Reprinted from O. Caldiran, H. Tan, and C. Basdogan, "An investigation of haptic perception of viscoelastic materials in the frequency domain," Apr. 2018.

From the experiments, Caldiran et al. concluded that the bounciness JND increased monotonically when increasing the phase. When considering Fu's experiments discussed before, at zero phase and $90\,\mathrm{deg}$ phase angle, Caldiran's experiments could be viewed as determining the damping JND and stiffness JND, respectively (with a constant magnitude response of the system). So the results seem to be consistent with the finding that stifness JND was larger than damping JND (imaginary $\approx 7.5\%$ and real $\approx 12\%$ part JND, respectively found by Fu et al. [26]) when the magnitude response of the system is kept constant. Furthermore, based on this research combined with the work of Fu it could be hypothesized that the JND area (area for which there is no perceived change in system dynamics) around a point in the imaginary plane might be elliptical. This possibility is also considered by Fu [26]. Caldiran's other experiment of firmness JND, however, does not support this theory as it shows no change in JND with increasing phase for constant magnitude. Furthermore, other studies show a lower stiffness JND [16] than damping JND [17], [30], which would imply an elliptical shape opposite to the one considered based on the first experiment. This contradiction is illustrated in Figures 3.6 to 3.8.

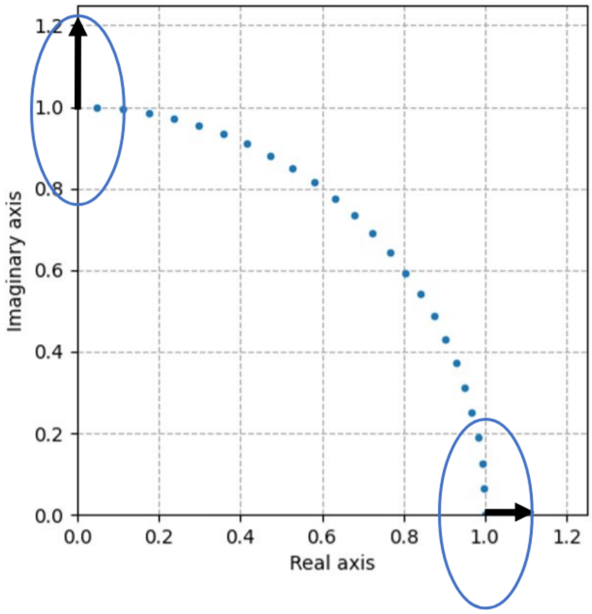

Figure 3.6: Showing the potential shapes of the JND area (defined as being the area around which no change in system dynamics is perceived) in the imaginary plane. This figure shows the ellipse considering Fu's JND experiments [26] and Caldiran's bounciness experiment [29].

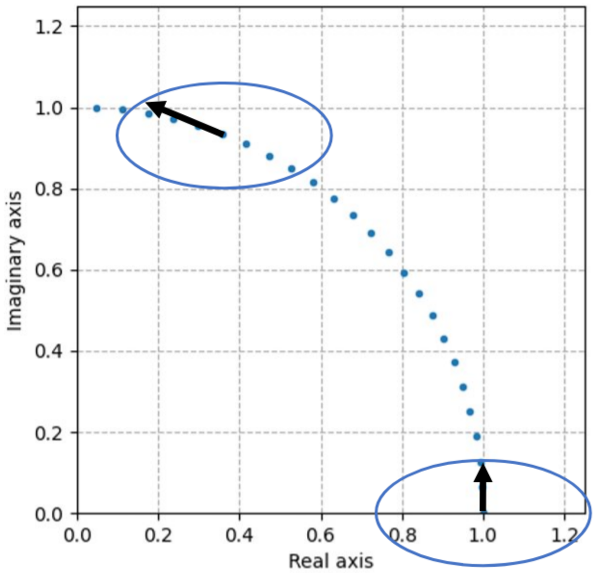

Figure 3.7: Showing the potential shapes of the JND area (defined as being the area around which no change in system dynamics is perceived) in the imaginary plane. This figure shows the elliptical JND area considering Jones et al. [16], [17] and Beauregard et al. [30].

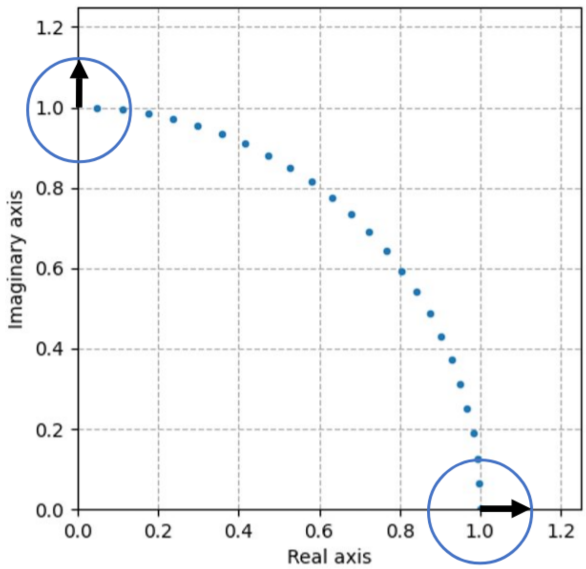

Figure 3.8: Showing the potential shapes of the JND area (defined as being the area around which no change in system dynamics is perceived) in the imaginary plane. This figure shows a circular JND area based on the results from the firmness experiment from Caldiran et al. [29]

4 Analytical Analysis and Hypothesis

Before constructing an hypothesis on the JND in friction in second order dynamics it is important to perform an analytical analysis of flight stick impedance considering a mass-spring-damper system with friction added. This chapter will discuss calculations of stick impedance under sinusoidal excitation. Analyses will be performed in both the the time domain as well as in the frequency domain. In the frequency domain the model of Fu, as discussed in Chapter 3, as well as the other literature, will be used to construct hypotheses of what a friction JND model could look like. These hypotheses will be discussed towards the end of this chapter.

4.1. Friction

Friction is defined as the force resisting the motion of two solid objects relative to each other [31]. There are different ways of modelling friction but the most common model identifies two nonlinear components. Static friction, which is the friction occurring at zero velocity, and dynamic friction, which is the friction to be considered when there is a non-zero velocity. When applying a force to an object with the purpose of sliding it over another object, initially, static friction will be the opposing force that is equal to the applied force until the motion starts. In motion, the static friction is considered zero and the dynamic friction, which is always lower accounts for the resistance caused by the interaction of the two surfaces. Figure 4.1 shows the different types of friction force as a function of velocity [32].

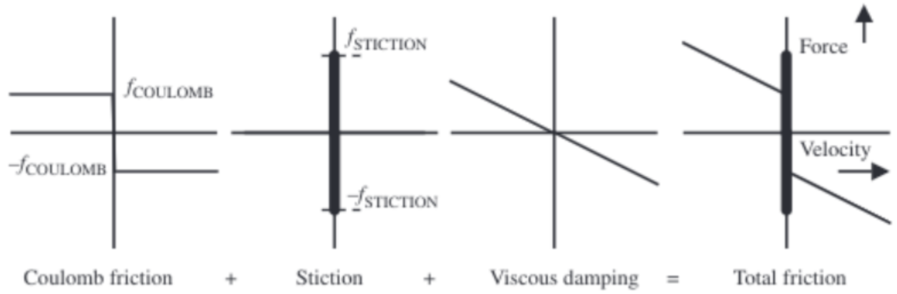

Figure 4.1: Model of friction, displaying friction force as a function of relative velocity between two objects. Reprinted from G. Ellis, “Chapter 12 - nonlinear behavior and time variation,” in Control System Design Guide (Fourth Edition), G. Ellis, Ed., Fourth Edition, Boston: Butterworth - Heinemann, 2012, pp. 249

In Figure 4.1, static friction is defined as $f_{stiction}$. Furthermore, viscous damping, which is a linear component is included as friction but for the purpose of this report will be named damping. When considering the moment of zero velocity there is an instantaneous shift from static friction to dynamic friction. In reality this shift is not instantaneous which is considered the Stribeck effect [32]. For a motion over a very short distance this moment of going from static to coulomb friction can be important. It may be difficult to move an object over a very short distance as friction decreases as soon as the motion starts which makes it difficult to stop in time and not overshoot the desired excitation [32]. For the purpose of this research the Stribeck effect will not be taken into account, since it is expected to have a small effect on the motions considered and therefore its role in perception will be negligible.

4.2. Impedance Calculations

The governing equation for the force-displacement relationship of a second order system including coulomb friction is given by Equation 4.1.

$$m\ddot{x}(t) + b\dot{x}(t) + f_c sign(\dot{x}) + kx(t) = F(t) \tag{4.1}$$

Equation 4.1 differs from Equation 3.1 in that it includes the signum function for adding dynamic friction (or coulomb friction). The dynamic friction f_c is defined as the dynamic friction coefficient f_{d_c} multiplied with the normal force F_n. For the purpose of this study the friction is assumed constant over the entire range of stick excitation. In reality, control column friction will slightly vary over the displacement angle [10], with a larger friction coefficient towards the maximum excitation. This effect, however, is limited, so for studying the JND in friction, modelling this friction as being constant over the entire range of the manipulator is appropriate. The signum function is mathematically defined as follows:

$$sign(x) = \begin{cases} -1 & x < 0 \\ 0 & x = 0 \\ 1 & x > 0 \end{cases} \tag{4.2}$$

As described in the previous section, static friction is defined as the friction occurring when there is zero velocity, so when $x = 0$ in Equation 4.2 and the dynamic friction is zero. Taking into account Equation 4.1 together with the static friction, Figure 4.2 shows stick impedance including friction under a sinusoidal excitation equivalent to Figure 3.1.

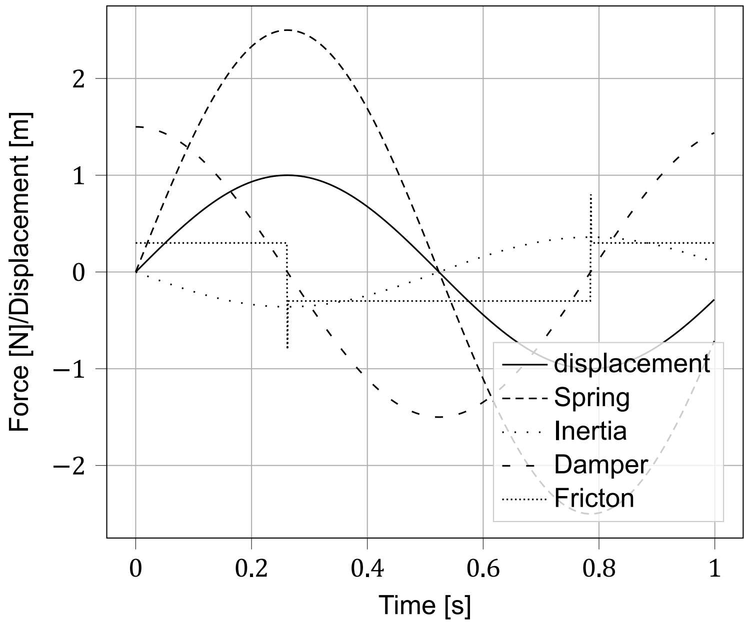

Figure 4.2: Force-Displacement (steady state) graph for typical second order system including friction ($k = 2.5$, $b = 0.25$, $m = 0.1$, $f_c = 0.3$)

When taking the combined spring, damping and inertia forces together, the graph in Figure 4.3 can be constructed. It shows the excitation force required for the sinusoidal excitation at $6\ [rad/s]$ for both the scenario without friction as well as including friction. It can be seen that, as expected, changing direction (a sign change in velocity) causes an instantaneous nonlinear jump in force.

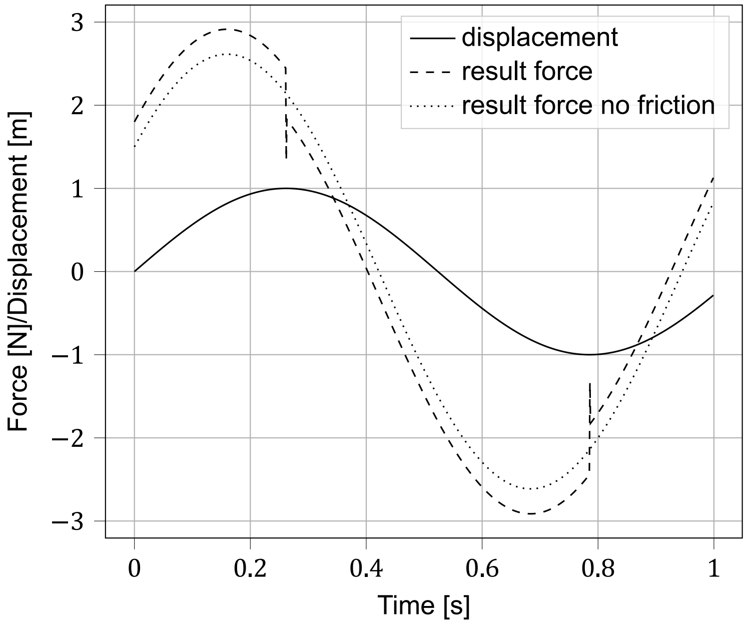

Figure 4.3: Force-Displacement (steady state) graph comparing scenario with and without friction ($k = 2.5$, $b = 0.25$, $m = 0.1$, $f_c = 0.3$)

4.3. Equivalent Dynamics

Fu's JND model, as described in Chapter 3, states that given a second order system as shown in Figure 4.3 ($H(j\omega)$), the JNDs in $\Im H(j\omega)$ and $\Re H(j\omega)$ will be directly proportional to the system's magnitude response. Eventhough $H(j\omega)$ has to be linear for this analysis, it is possible to define the linear equivalent dynamics. These equivalent dynamics approximate the nonlinear system including friction. When looking at Figure 4.3 and disregarding the nonlinear jumps, it can be observed that friction increases the magnitude response of the system without changing its phase response. Calculating this equivalent system $H(j\omega)_{eq}$ is relatively straightforward as shown in Equations 4.3 and 4.4. The second order system with an increased magnitude response can be seen in Figure 4.4.

$$\Re H(j\omega) = k - m\omega^2,\ \Im H(j\omega) = b\omega j \tag{4.3}$$

$$|H(j\omega)|_{eq} = |H(j\omega)| + f_c = \sqrt{\Re H(j\omega)^2 + \Im H(j\omega)^2} + f_c \tag{4.4}$$

Also the imaginary plane representation can then be calculated using Equation 4.5 and 4.6. Figure 4.5 shows the equivalent dynamics in the imaginary plane.

$$\Re H(j\omega)_{eq} = |H(j\omega)|_{eq} \cdot cos(\angle H(j\omega)) = |H(j\omega)|_{eq} \cdot cos(atan(\frac{\Im H(j\omega)}{\Re H(j\omega)})) \tag{4.5}$$

$$\Im H(j\omega)_{eq} = |H(j\omega)|_{eq} \cdot sin(\angle H(j\omega)) = |H(j\omega)|_{eq} \cdot sin(atan(\frac{\Im H(j\omega)}{\Re H(j\omega)})) \tag{4.6}$$

When comparing the equivalent dynamics linear system with the nonlinear system with friction the main difference occurs when the sinusoidal motion changes direction. This is when the friction force changes direction and there is a instantaneous drop in force (in either direction). So when considering a sinusoidal excitation only, there are two factors which can play a role in perceiving a change in system dynamics.

The first is the change in magnitude response, as described by the equivalent system dynamics. The perception of this change in dynamics can be analyzed according to the model by Fu [26], as it is described linearly. The model could ultimately be used to describe the JND in friction if the equivalent dynamics magnitude response is the determinant factor when perceiving changes in friction.

The second factor that can play a role in the perception of changes in system impedance when friction is included is the nonlinear force drop. Compared to the equivalent dynamics this factor is more

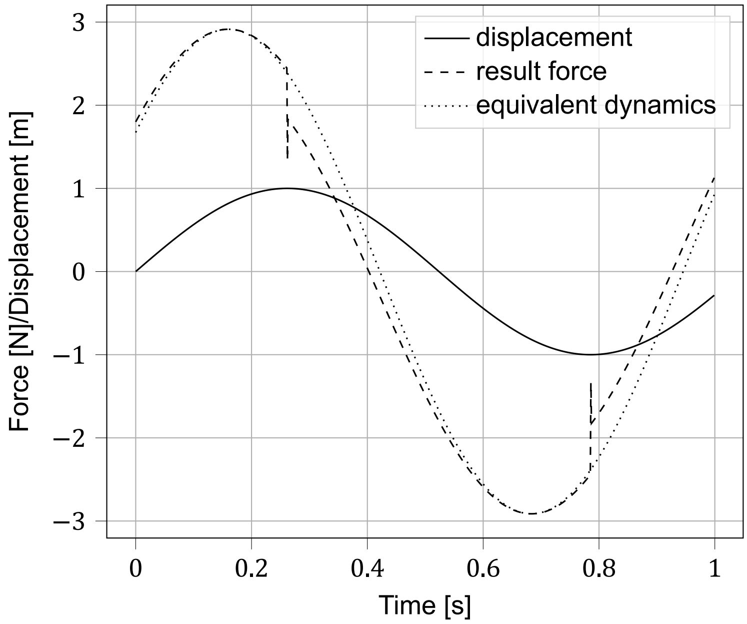

Figure 4.4: Force-Displacement (steady state) graph with scenario including friction and the equivalent linear dynamics $H(j\omega)_{eq}$

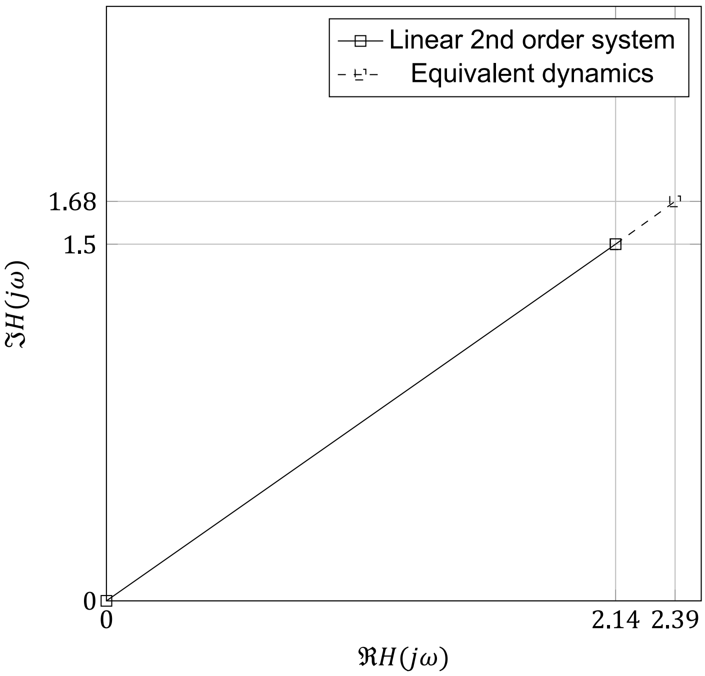

Figure 4.5: Imaginary plane representation of the original system without friction and the equivalent linear dynamics $H(j\omega)_{eq}$ of the system with friction

complex as it can not be described by a linear model. When looking at this force drop as a determinant factor for perceiving changes in friction, it is important to consider the effect of $\Re H(j\omega)_{friction}$ and $\Im H(j\omega)_{friction}$ ($H(j\omega)_{friction}$ is the system $H(j\omega)$ with friction added) on this force drop.

An interactive plotting program is used (as found in appendix A) to visually examine the effect of $\Re H(j\omega)_{friction}$ and $\Im H(j\omega)_{friction}$ on the force drop. It was found that $\Re H(j\omega)_{friction}$ affects the force offset at which the force-drop occurs as well as its phase lag. This is to be expected considering the force-drop occurs at zero velocity so the imaginary part of the system's response is zero at that moment. The larger $\Re H(j\omega)_{friction}$, the greater the force at which the direction change of the sinusoidal motion occurs. On the other hand, the imaginary part $\Im H(j\omega)_{friction}$ does not influence the force at which the direction changes (as damping is always zero at this moment) but does influence the phase as well. The excitation frequency, however, does influence this force-drop timing independent of other system parameters since it increases the system's phase through the increased damping and inertia at higher frequencies. Figure 4.6, Figure 4.7, Figure 4.8 and Figure 4.9 show how the real and imaginary parts of $H(j\omega)_{friction}$ affect the force-displacement relationship of the system with friction and the effect on the timing of the nonlinear force drop.

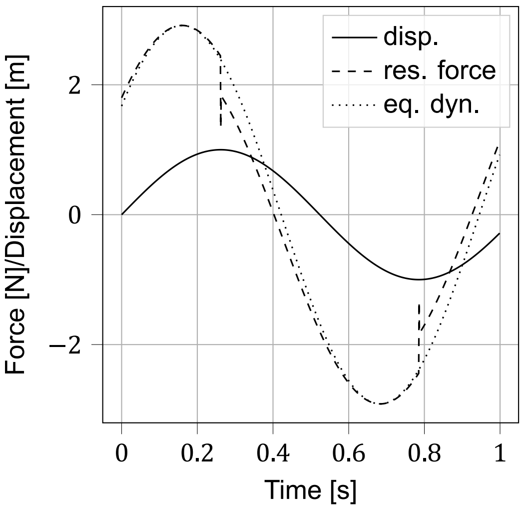

Figure 4.6: Showing the force-displacement graph of a sinusoidal excitation while changing the $\Re H(j\omega)_{friction}$, here $k = 2.5$

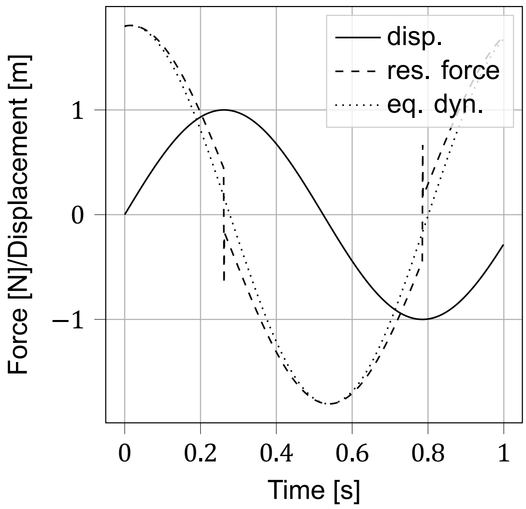

Figure 4.7: Showing the force-displacement graph of a sinusoidal excitation while changing the $\Re H(j\omega)_{friction}$, here $k = 0.5$

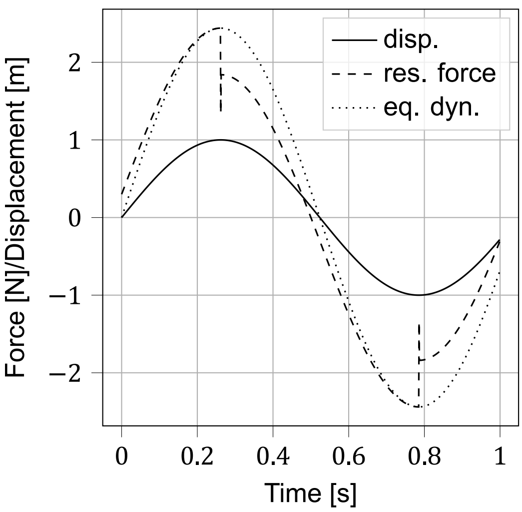

Figure 4.8: Showing the force-displacement graph of a sinusoidal excitation while changing the $\Im H(j\omega)_{friction}$, here $b = 0$

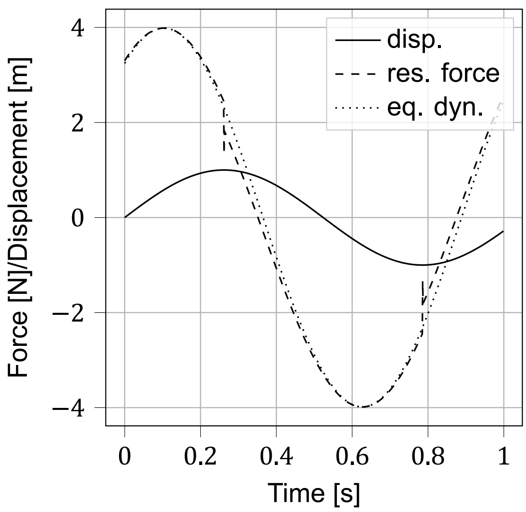

Figure 4.9: Showing the force-displacement graph of a sinusoidal excitation while changing the $\Im H(j\omega)_{friction}$, here $b = 0.5$

Furthermore, aside from the effect of the real and imaginary parts of $H(j\omega)$ on the force-drop in the force-displacement graphs, frequency might also play an important role in the perception of friction. The sharp force-drop when changing the direction of movement can be seen as a change in force at very high (almost infinite) frequency. When increasing the excitation frequency the force-drop as a sudden increase in frequency could be masked by an already high frequency. This frequency dependence of friction perception is illustrated in Figure 4.10 and 4.11. It can be seen that even though the magnitude response of the system does not change significantly, the higher frequency motion may have a masking effect on the friction perception.

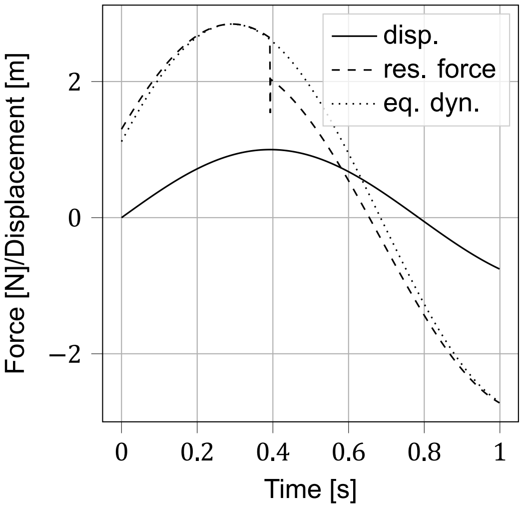

Figure 4.10: Showing the force-displacement graph of a sinusoidal excitation while changing the excitation frequency, here $\omega = 4$

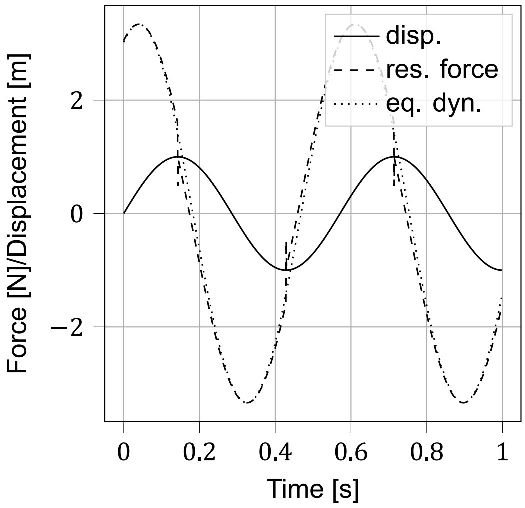

Figure 4.11: Showing the force-displacement graph of a sinusoidal excitation while changing the excitation frequency, here $\omega = 11$

4.4. Hypotheses

It was found by Samur et al. [21] that when just considering friction without other dynamics Weber's law holds and the friction JND is proportional to the reference level of friction. Therefore a first hypothesis for the friction JND, assuming no effect from the presence of second order dynamics, is the following:

1. Friction JND is proportional to the reference friction setting.

However, it is likely that the second order dynamics will have a masking effect on the perception of friction and also the friction JND. Therefore, additional hypotheses are necessary for the more specific case where friction is added to second order dynamics.

Summarizing this chapter, there are two approaches when looking at friction perception in the presence of second order dynamics when performing a sinusoidal excitation. They both lead to their own hypothesis on the friction JND in the presence of second order dynamics.

The first approach considers the equivalent dynamics and applies Fu's linear JND model [26] to determine the JNDs in friction. In this case the change in magnitude response of the equivalent dynamics system dictates whether a change in friction is perceived and also if friction is perceived at all (compared to the same system without friction). For this approach the hypothesis of friction JND in the presence of second order dynamics under sinusoidal excitation is formulated as follows:

2. Friction JND is proportional to the magnitude response of the equivalent dynamics system $H(j\omega)_{eq}$.

For the second approach it is argued that friction perception depends on the real or imaginary parts of the system, on the excitation frequency or on any combination of these. Based on Weber's law on force JNDs it can be hypothesized that when considering the sinusoidal excitation the perception of the sudden force-drop depends heavily on the force at which this force-drop occurs. This is because differences in force, which is what is to be perceived when perceiving different force-drops, are perceived better at lower reference forces. As explained before, the real part (stiffness and mass) of the system's response is responsible for this force occurring at the direction change.

Also, the friction JND could depend on the gradient of the force-displacement graph at the moment of direction change. This gradient, defined as the time derivative of the resultant force on the stick at the moment of direction change, can be influenced by the phase response of the system $H(j\omega)$ as well as the excitation frequency.

Both scenarios of changing the offset force at which the nonlinear force-drop occurs and changing the gradient could mask the force-drop, meaning the equivalent dynamics system and the nonlinear system with friction would be indistinguishable. In this case, JNDs in friction are expected to follow hypothesis 2. However, if the force-drop does have an effect, it could potentially lower the friction JND. This is because the perception of this non-linearity would add to the perception of increased magnitude response that friction causes and either one could be the determining factor for the JND in friction depending on the properties of the force-drop. Considering phase-lags close to $90°$ and lower excitation frequencies it is possible that it is not the equivalent system's magnitude response that determines the friction JND. The following hypothesis considers this possibility:

3. Friction JND is influenced by the masking second order system's frequency or phase independently of its magnitude response

5 Experiment

In this chapter the proposed experiment is discussed. The experimental setup and conditions follow from the research questions given in the Introduction and the hypotheses as formulated in Chapter 4. Firstly, the equipment and techniques will be discussed, following an explanation of the experiment conditions and procedures. Finally, a calculation of the proper subject size is presented in the last section of this chapter.

5.1. Experiment Apparatus

The experiments will be performed in the Human-Machine Laboratory at the Faculty of Aerospace Engineering, TU Delft. The device and experiment setup is shown in Figure 3.3. The manipulator is an admittance-controlled side-stick, driven by an electro-hydraulic motor. The manipulator will be limited to 1 DoF, only being able to move in the left or right (lateral) direction. Between different trials, the manipulator can be adjusted in stiffness, mass and damping parameters, as well as friction (dynamic and static). A noise-cancelling headphone will be used to cancel out any potential auditory feedback that could help in identifying different manipulator settings. Furthermore, an LCD screen in front of the test subjects will provide the necessary visual cues.

Since test subjects will be required to give feedback on the manipulator impedance setting, it is important that they are familiarized with the haptic display before starting any experiment. For studying friction perception this means in practice that test subjects should be given clear examples of what different levels of friction feel like, also in the presence of different second order system dynamics. With differences in friction far above the JND subjects should be taught what more and less friction feels like.

5.2. Controlled Excitation Experiment

Since this thesis follows up on the work of Fu et al. [9], the experiment follows a similar protocol to their JND experiments [26]. Test subjects will perform a preview tracking task which will be a sinusoidal motion with a constant frequency within one trial. A sinusoidal tracking task is used as it allows for a frequency domain analysis. Furthermore, considering the relevance of this research with the aim to give a more scientific basis for CLS transparency requirements, a sinusoidal tracking task makes sense also from this perspective as a pilot's control inputs can be said to more or less approximate a multisine. A single frequency, sinusoidal tracking task is the most simplest of tasks and therefore the resulting JNDs will be conservative estimates with regards to real flight tasks. In reality, pilots will perform more complex controlling tasks which could lead to higher JNDs. Looking at the JNDs in friction when performing a very simple tracking task will most likely result in a relatively low JND. As discussed before, it is possible that certain motor skills, developping based on the haptic feedback of the CLS, develop unconsciously. Therefore, it could be argued that this aim to find this lowest JND is not only conservative but actually it is a necessity.

To determine the friction JNDs a one-up/two down adaptive staircase procedure will be used as described in Chapter 2.2 and more extensively by Kingdom et al. [33]. When considering the hypotheses, several second order system configurations and levels of reference friction can be formulated for which the JND in friction should be determined.

The first hypothesis considers the friction JND independent of the second order system dynamics. To test this hypothesis, three different levels of friction are considered for the same mass-spring-damper configuration in a 6 [rad/s] preview tracking task. For each friction setting the JND in friction will be determined while the other stick dynamics (mass, spring and damper) will be constant and representative for common flight stick dynamics. Figure 5.1 gives an imaginary plane representation of these first three conditions while in Table 5.1 all stick impedance parameters are given.

The second hypothesis assumes a relationship between friction JND and the second order system's magnitude response. To test this hypothesis the magnitude response $|H(j\omega)|$ of the mass-spring-damper system will be varied with respect to the first three experiments by $+/-25\%$. Re-using condition 2, it is possible to compare the friction JND for three different values of $|H(j\omega)|$ by adding condition 4 and 5 as shown in Figure 5.2 and Table 5.1.

Finally, the third hypothesis considers the possibility either the second order system's phase response or excitation frequency might influence the friction JND. To examine both effects independently of the system's magnitude response conditions 6, 7, 8 and 9 are added. For conditions 6 and 7 the excitation frequency (the frequency of the tracking task) is varied to include both 3 [rad/s] and 8 [rad/s] while $|H(j\omega)|$ is kept constant. Conditions 8 and 9 are performed at the same frequency of 6 [rad/s] but this time the second order system's phase is varied while also keeping $|H(j\omega)|$ constant. As for condition 4 and 5, again condition 2 is re-used to have three levels of excitation frequency and phase to compare. The imaginary plane representation of conditions 6 to 9 is given by Figure 5.3 and all parameter values can be found in Table 5.1.

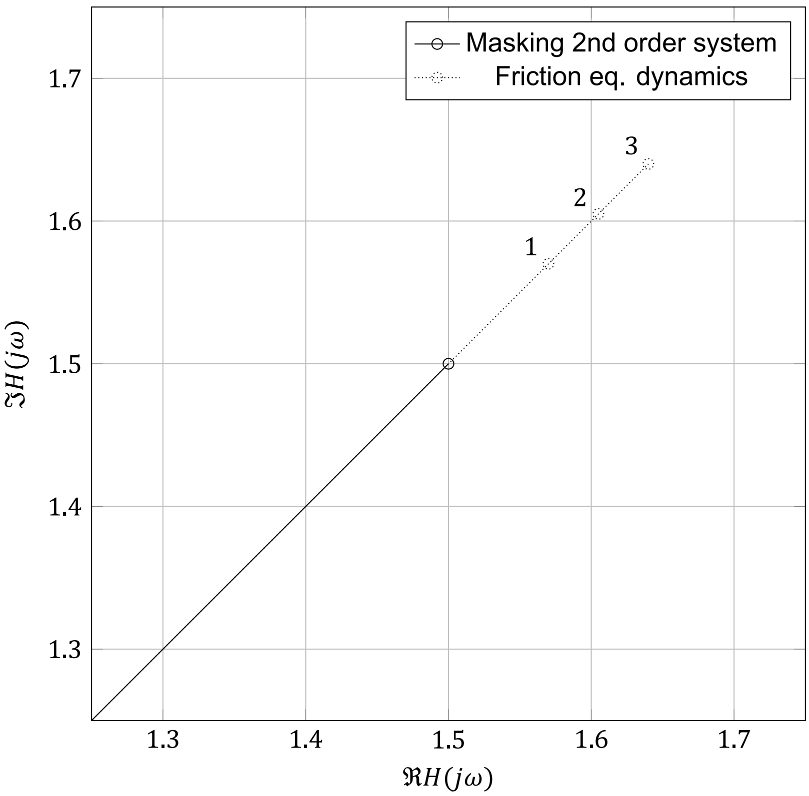

Figure 5.1: Imaginary plane representation experiment conditions 1-3

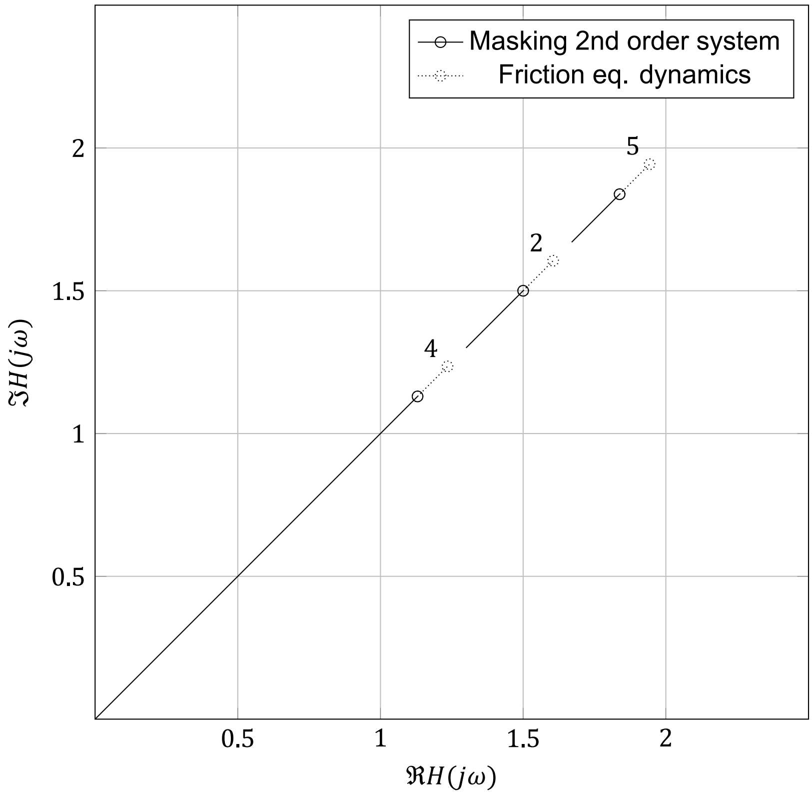

Figure 5.2: Imaginary plane representation experiment conditions 4,5

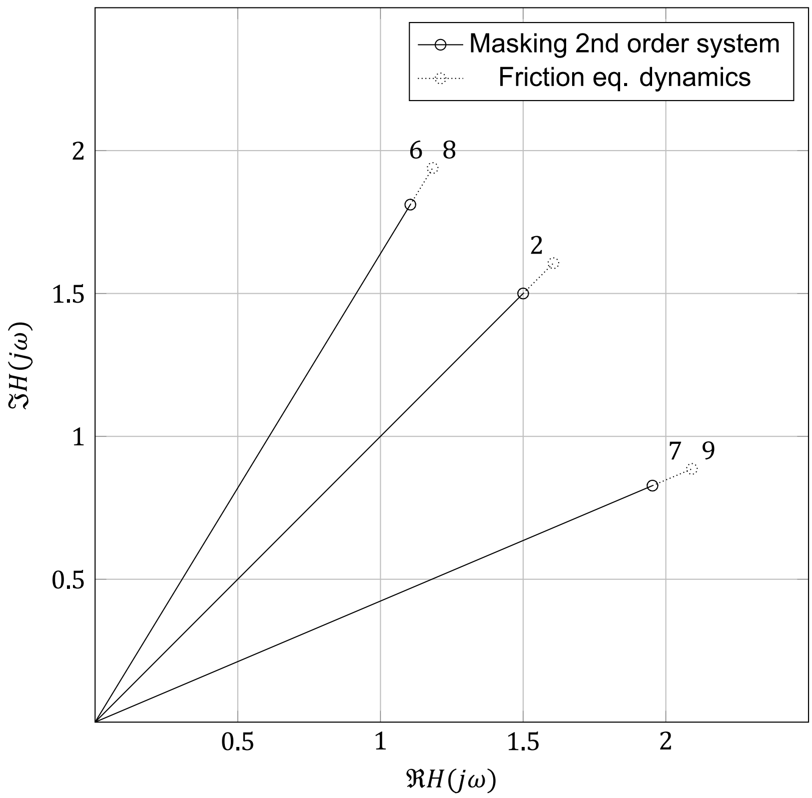

Figure 5.3: Imaginary plane representation experiment conditions 6-9

Table 5.1: Experiment conditions parameters

Experiment Condition	Friction $[Nm]$	Freq. $[rad/s]$	$\lvert H(j\omega)\rvert$	$\Re(H(j\omega))$	$\Im(H(j\omega))$	Stiffness $[Nm/rad]$	Mass $[kgm^2]$	Damping $[Nms/rad]$
1	0.1	6	2.12	1.5	1.5	1.87	0.01	0.25
2	0.15	6	2.12	1.5	1.5	1.87	0.01	0.25
3	0.2	6	2.12	1.5	1.5	1.87	0.01	0.25
4	0.15	6	1.6	1.13	1.13	1.49	0.01	0.19
5	0.15	6	2.6	1.84	1.84	2.2	0.01	0.31
6	0.15	8	2.12	1.10	1.81	1.74	0.01	0.23
7	0.15	3	2.12	1.95	0.83	2.04	0.01	0.28
8	0.15	6	2.12	1.10	1.81	1.46	0.01	0.3
9	0.15	6	2.12	1.95	0.83	2.31	0.01	0.14

5.3. Subject Size

For analyzing differences in JNDs under different experiment conditions, a one-way repeated measures ANOVA will be performed. For this statistical analysis the dependent measure will be the friction JND and the independent variable will be the different experiment conditions, varied by changing reference friction and second order system impedance setting. Each participant will be tested under all experiment conditions, so the groups for different experiment conditions include the same subjects, which is an important condition for a one-way repeated measures ANOVA.

When determining the proper subject size for the experiments, one of the main considerations is the variation in JNDs when measuring them for different test subjects. However, before conducting the experiment it is difficult to predict these variances. From previous research carried out by Fu et al. [26], [34] it is possible to estimate potential effect sizes, i.e., changes in the JND under different experiment conditions, and also see how JNDs vary among participants. Using $G^{*}Power$ [35], the necessary subject size can be determined based on the required power and effect size.

In one of his papers [28], Fu describes two experiments where the Weber fractions for stiffness JND and damping JND are measured under different experiment conditions. Both experiments demonstrate how the Weber fractions can change significantly, adding stiffness to a damping JND experiment can easily double the Weber fraction for damping JND, showing how significant these masking effects can be. With the null-hypothesis of assuming constant Weber fractions for both stiffness JND and damping JND, Fu gives a very strong statistical proof of the masking effect of stiffness on damping JND and mass on stiffness JND.

For Fu's damping JND experiment [28] the effect size can be calculated from the raw measurement data. Cohen's f (effect size) is then calculated to be 0.90 and with his subject size of eight the power of his study was as high as 0.99, calculated using $G^{*}Power$.

For the current research, different statistical tests will be performed, comparing at least three different experiment conditions. To be conservative in the subject size calculation it is assumed that the effect size of the second order system masking the friction JND is at least 0.45, which is half of what was calculated for Fu's damping experiment [28]. Then using $G^{*}Power$, assuming sphericity and a correlation among repeated measures of 0.5, for a power of 0.9, a subject size of 10 is required. Considering the conservative effect size and relatively large power of 0.9, for this research it is chosen that a subject size of 10 will be more than sufficient to find a masking effect of the second order system dynamics on friction JND, if it exists.

A

Impedance Visualization Tool

```python
import sys
import PyQt5.QtCore as QtCore

from PyQt5.QtCore import Qt
from PyQt5.QtWidgets import QApplication, QHBoxLayout, QLabel, QSizePolicy, QSlider, \
    QSpacerItem, QCheckBox, \
    QVBoxLayout, QWidget

import pyqtgraph as pg
import numpy as np

from scipy import signal


class Slider(QWidget):
    def __init__(self, minimum, maximum, name="unknown", parent=None):
        super(Slider, self).__init__(parent=parent)
        self.verticalLayout = QVBoxLayout(self)
        self.label = QLabel(self)
        self.label_name = QLabel(self)
        self.label_name.setText(name)
        self.verticalLayout.addWidget(self.label_name)
        self.verticalLayout.addWidget(self.label)
        self.horizontalLayout = QHBoxLayout()
        spacerItem = QSpacerItem(0, 20, QSizePolicy.Expanding, QSizePolicy.Minimum)
        self.horizontalLayout.addItem(spacerItem)
        self.slider = QSlider(self)
        self.slider.setOrientation(Qt.Vertical)
        self.horizontalLayout.addWidget(self.slider)
        spacerItem1 = QSpacerItem(0, 20, QSizePolicy.Expanding, QSizePolicy.Minimum)
        self.horizontalLayout.addItem(spacerItem1)
        self.verticalLayout.addLayout(self.horizontalLayout)
        self.resize(self.sizeHint())

        self.minimum = minimum
        self.maximum = maximum
        self.slider.valueChanged.connect(self.setLabelValue)
        self.x = None
        self.setLabelValue(self.slider.value())

    def setLabelValue(self, value):
        self.x = self.minimum + (float(value) / (
            self.slider.maximum() - self.slider.minimum())) * (self.maximum - self.minimum)
        self.label.setText("{:.2f}".format(self.x))


class Widget(QWidget):
    def __init__(self, parent=None):
        super(Widget, self).__init__(parent=parent)
        self.horizontalLayout = QHBoxLayout(self)
```

```
        self.horizontalLayout.setSpacing(0)
        self.w1 = Slider(0, 5, "Stiff.")
        self.horizontalLayout.addWidget(self.w1)

        self.w2 = Slider(0, 0.7, "Damp.")
        self.horizontalLayout.addWidget(self.w2)

        self.w3 = Slider(-0, 0.05, "Mass")
        self.horizontalLayout.addWidget(self.w3)

        self.w4 = Slider(0, 30, "Freq.")
        self.horizontalLayout.addWidget(self.w4)

        self.w6 = Slider(0, 1, "Dyn. Fric.")
        self.horizontalLayout.addWidget(self.w6)

        self.w7 = Slider(0, 0.5, "Stat. Fric.")
        self.horizontalLayout.addWidget(self.w7)

        self.w5 = QVBoxLayout(self)
        self.checkboxfriction = QCheckBox("Fric.", self)
        self.w5.addWidget(self.checkboxfriction)
        self.horizontalLayout.addItem(self.w5)
        self.checkboxfriction.stateChanged.connect(self.update_plot2)
        self.checkboxfriction.stateChanged.connect(self.update_plot)

        self.w5.addStretch()

        self.win = pg.GraphicsWindow(title="Basic plotting examples")
        self.horizontalLayout.addWidget(self.win)
        self.p6 = self.win.addPlot(title="Imaginary Plane")
        self.p6.addLegend()
        self.curve = self.p6.plot(pen=pg.mkPen('r', width=3))
        self.curve4 = self.p6.plot(symbolPen='r', symbolBrush='r', symbol='o')
        self.curve6 = self.p6.plot(
            pen=pg.mkPen('y', width=2, style=QtCore.Qt.DashLine), name="eq. dynamics")
        self.curve7 = self.p6.plot(symbolPen='y', symbolBrush='y', symbol='o')
        self.p6.setXRange(-5, 5, padding=0)
        self.p6.setYRange(-5, 5, padding=0)
        self.p6.showGrid(x=True, y=True, alpha=0.3)
        self.update_plot()

        self.win2 = pg.GraphicsWindow(title="Basic plotting examples")
        self.horizontalLayout.addWidget(self.win2)
        self.p7 = self.win2.addPlot(title="Force/Displacement")
        self.p7.addLegend()
        self.curve2 = self.p7.plot(pen='r', name="resultant force")
        self.curve3 = self.p7.plot(pen=pg.mkPen('b', width=2), name="displacement")
        self.curve5 = self.p7.plot(
            pen=pg.mkPen('r', width=0.5, style=QtCore.Qt.DashLine), name="no friction")
        self.curve8 = self.p7.plot(
            pen=pg.mkPen(
                'y', width=0.5, style=QtCore.Qt.DashLine), name="equivalent system")
        self.p7.setXRange(0, 1, padding=0)
        self.p7.setYRange(-5, 5, padding=0)
        self.p7.showGrid(x=True, y=True, alpha=0.3)
        self.update_plot2()

        self.w1.slider.valueChanged.connect(self.update_plot)
        self.w2.slider.valueChanged.connect(self.update_plot)
        self.w3.slider.valueChanged.connect(self.update_plot)
        self.w4.slider.valueChanged.connect(self.update_plot)
        self.w6.slider.valueChanged.connect(self.update_plot)
        self.w7.slider.valueChanged.connect(self.update_plot)

        self.w1.slider.valueChanged.connect(self.update_plot2)
        self.w2.slider.valueChanged.connect(self.update_plot2)
        self.w3.slider.valueChanged.connect(self.update_plot2)
        self.w4.slider.valueChanged.connect(self.update_plot2)
        self.w6.slider.valueChanged.connect(self.update_plot2)
        self.w7.slider.valueChanged.connect(self.update_plot2)
```

```

    def update_plot(self):
        Fn = 1
        k = self.w1.x # spring constant Nm/rad
        b = self.w2.x # damping constant Nms/rad
        m = self.w3.x # mass
        omega = self.w4.x # frequency

        real = k-(m*omega**2)
        imag = b*omega
        phase = np.arctan2(imag, real)
        x_range = np.arange(0, real, 0.01)
        data = x_range*phase
        self.curve.setData(x=[0, real], y=[0, imag])
        self.curve4.setData(x=[real], y=[imag])
        print("real=", real)
        print("imaginary=", imag)
        print("phase=", phase)

        mag = np.sqrt(real**2 + imag**2)
        if self.checkboxfriction.checkState():
            mag_new = mag + self.w6.x * Fn
            real_new = mag_new * np.cos(phase)
            imag_new = mag_new * np.sin(phase)
            self.curve6.setData(x=[0, real_new], y=[0, imag_new])
            self.curve7.setData(x=[real_new], y=[imag_new])
            print(mag_new)
            print(real_new)
            print(imag_new)
        else:
            self.curve6.clear()
            self.curve7.clear()


    def update_plot2(self):
        freq = self.w4.x # in radians

        # x-grid
        x_range = np.arange(0, 1, 0.001)

        # Using  the tracking task the displacement is given as a 6 rad/s sinusoid
        y_disp = np.sin(freq*x_range) # y_disp is defined in radians
        y_vel = freq*(np.cos(freq*x_range))
        y_acc = (freq**2)*y_disp

        k = self.w1.x # spring constant Nm/rad
        b = self.w2.x # damping constant Nms/rad
        m = self.w3.x # mass
        u_d = self.w6.x # dynamic friction constant
        u_s = self.w7.x # static friction constant
        Fn = 1 # normal force (friction)

        y_force_stiffness = k*y_disp
        y_force_inertia = -m*y_acc
        y_force_damping = b*y_vel

        # Now for friction we can use the signum function
        # It should be noted we are assuming coulomb friction
        y_force_friction = u_d*Fn*np.sign(y_vel)

        y_force_friction_static = u_s*Fn

        # find indices of static friction
        static_indp = np.where(np.sign(y_vel)[:-1] < np.sign(y_vel)[1:])[0] + 1
        static_indn = np.where(np.sign(y_vel)[:-1] > np.sign(y_vel)[1:])[0] + 1
        print(static_indp)
        print(static_indn)

        # create static friction array
        # for all positive and negative indices create an array and add it to the previous
        y_force_friction_stat = np.zeros(len(x_range))
```

```
        for i in static_indp:
            y_force_friction_stat += y_force_friction_static* \
                signal.unit_impulse(len(x_range), i)

        for i in static_indn:
            y_force_friction_stat += -y_force_friction_static* \
                signal.unit_impulse(len(x_range), i)

        # Combined forces
        y_force_comb_nofriction = y_force_stiffness + \
            y_force_inertia +y_force_damping

        y_force_comb = y_force_stiffness + y_force_friction + \
        y_force_friction_stat + y_force_inertia +y_force_damping

        print(self.checkboxfriction.checkState())

        if self.checkboxfriction.checkState():
            data = y_force_comb
            data2 = y_force_comb_nofriction
            self.curve5.setData(x=x_range, y=data2)
        else:
            data = y_force_comb_nofriction
            self.curve5.clear()

        self.curve2.setData(x=x_range, y=data)
        self.curve3.setData(x=x_range, y=np.sin(freq*x_range))

        if self.checkboxfriction.checkState():
            real = k-(m*freq**2)
            imag = b*freq
            phase = np.arctan2(imag, real)
            mag = np.sqrt(real**2 + imag**2)
            mag_new = mag + self.w6.x * Fn
            real_new = mag_new * np.cos(phase)
            imag_new = mag_new * np.sin(phase)
            # determine res force of mass/spring damper using real and imag parts
            data = mag_new * np.sin(freq*x_range + phase)
            self.curve8.setData(x=x_range, y=data)
        else:
            self.curve8.clear()

if __name__ == '__main__':
    app = QApplication(sys.argv)
    w = Widget()
    w.show()
    sys.exit(app.exec_())
```

Listing A.1: python code using pyqt library

Bibliography

[1] T. B. Sheridan, “Telerobotics,” *Automatica*, vol. 25, no. 4, pp. 487–507, 1989.

[2] S. Avgousti, E. Christoforou, A. Panayides, S. Voskarides, C. Novales, L. Nouaille, C. Pattichis, and P. Vieyres, “Medical telerobotic systems: Current status and future trends,” *BioMedical Engineering OnLine*, vol. 15, Aug. 2016. DOI: `10.1186/s12938-016-0217-7`.

[3] T. Fong, J. Zumbado, N. Currie-Gregg, A. Mishkin, and D. Akin, “Space telerobotics: Unique challenges to human-robot collaboration in space,” *Reviews of Human Factors and Ergonomics*, vol. 9, pp. 6–56, Dec. 2013. DOI: `10.1177/1557234X13510679`.

[4] EASA, “CS-FSTD(A): Certification specifications for aeroplane flight simulation training,” Tech. Rep., May 2018.

[5] FAA, “14 CFR Part 60: Flight simulation training device initial and continuing qualification and use,” Tech. Rep., Oct. 2016.

[6] N. Dahlstrom, S. Dekker, R. van Winsen, and J. Nyce, “Fidelity and validity of simulator training,” *Theoretical Issues in Ergonomics Science*, vol. 10, no. 4, pp. 305–314, 2009. DOI: `10.1080/14639220802368864`. eprint: `https://doi.org/10.1080/14639220802368864`. [Online]. Available: `https://doi.org/10.1080/14639220802368864`.

[7] F. Gabbiani and S. J. Cox, “Chapter 28 - relating neuronal responses and psychophysics,” in *Mathematics for Neuroscientists (Second Edition)*, F. Gabbiani and S. J. Cox, Eds., Second Edition, San Diego: Academic Press, 2017, pp. 463–473, ISBN: 978-0-12-801895-8. DOI: `https://doi.org/10.1016/B978-0-12-801895-8.00028-2`. [Online]. Available: `https://www.sciencedirect.com/science/article/pii/B9780128018958000282`.

[8] G. Fechner, *Elemente der Psychophysik*. Breitkof und Hartel, 1860.

[9] W. Fu, “Evidence - based development and evaluation of haptic interfaces for manual control,” Ph.D. dissertation, TU Delft, 2019.

[10] W. Fu, personal communication [email], Nov. 18, 2020.

[11] T. Editors of Encyclopaedia Brittanica, *Weber’s law*, Jan. 2020. [Online]. Available: `https://www.britannica.com/science/Webers-law`.

[12] A. M. Colman, *A Dictionary of psychology*, eng. Oxford: Oxford University Press, 2001, ISBN: 0198662114.

[13] R. H. Wozniak, “Introduction to elemente der psychofysik gustav theodor fechner (1860),” *Classics in Psychology, 1855-1914: Historical essays*, 1999.

[14] Nutter and W. J. Forrest, *Weber-fechner law*, 2010. [Online]. Available: `https://lib.dr.iastate.edu/plantpath_pubs/71/`.

[15] B. Treutwein, “Adaptive psychophysical procedures,” *Vision Research*, vol. 35, no. 17, pp. 2503–2522, 1995, ISSN: 0042-6989. DOI: `https://doi.org/10.1016/0042-6989(95)00016-X`. [Online]. Available: `https://www.sciencedirect.com/science/article/pii/004269899500016X`.

[16] L. A. Jones and I. W. Hunter, “A perceptual analysis of stiffness,” *Experimental Brain Research*, vol. 79, pp. 150–156, 1990. DOI: `https://doi.org/10.1007/BF00228884`.

[17] ——, “A perceptual analysis of viscosity,” *Experimental Brain Research*, vol. 94, pp. 343–351, 1993. DOI: `https://doi.org/10.1007/BF00230304`.

[18] B. M. Haas, E. Bergström, A. Jamous, and A. Bennie, “The inter rater reliability of the original and of the modified ashworth scale for the assessment of spasticity in patients with spinal cord injury,” *Spinal Cord*, vol. 34, no. 9, pp. 560–564, Sep. 1996, ISSN: 1476-5624. DOI: `10.1038/sc.1996.100`. [Online]. Available: `https://doi.org/10.1038/sc.1996.100`.

[19] J. F. M. Fleuren, G. E. Voerman, C. V. Erren-Wolters, G. J. Snoek, J. S. Rietman, H. J. Hermens, and A. V. Nene, "Stop using the ashworth scale for the assessment of spasticity," *Journal of Neurology, Neurosurgery & Psychiatry*, vol. 81, no. 1, pp. 46–52, 2010, ISSN: 0022-3050. DOI: 10.1136/jnnp.2009.177071. eprint: https://jnnp.bmj.com/content/81/1/46.full.pdf. [Online]. Available: https://jnnp.bmj.com/content/81/1/46.

[20] W. B. Messaoud, M.-A. Bueno, and B. Lemaire-Semail, "Relation between human perceived friction and finger friction characteristics," *Tribology International*, vol. 98, pp. 261–269, 2016, ISSN: 0301-679X. DOI: https://doi.org/10.1016/j.triboint.2016.02.031. [Online]. Available: https://www.sciencedirect.com/science/article/pii/S0301679X1600116X.

[21] E. Samur, J. Colgate, M. Peshkin, B. Rogowitz, and T. Pappas, "Psychophysical evaluation of a variable friction tactile interface," Jan. 2009.

[22] D. Gueorguiev, E. Vezzoli, A. Mouraux, B. Lemaire-Semail, and J. L. Thonnard, "The tactile perception of transient changes in friction," *J R Soc Interface*, vol. 14, no. 137, Dec. 2017.

[23] W. Tang, R. Liu, Y. Shi, C. Hu, S. Bai, and H. Zhu, "From finger friction to brain activation: Tactile perception of the roughness of gratings," *Journal of Advanced Research*, vol. 21, pp. 129–139, 2020, ISSN: 2090-1232. DOI: https://doi.org/10.1016/j.jare.2019.11.001. [Online]. Available: https://www.sciencedirect.com/science/article/pii/S2090123219301791.

[24] M. M. van Paassen, *Ae4322 reference: Control loading systems*, 2018.

[25] ——, personal communication, May 17, 2021.

[26] W. Fu, M. M. van Paassen, and M. Mulder, "Human threshold model for perceiving changes in system dynamics," *IEEE Transactions on Human-Machine Systems*, vol. PP, Apr. 2020. DOI: 10.1109/THMS.2020.2989383.

[27] M. Rank, T. Schauss, A. Peer, S. Hirche, and R. Klatzky, "Masking effects for damping jnd," Jun. 2012, pp. 145–150. DOI: 10.1007/978-3-642-31404-9_25.

[28] W. Fu, A. Landman, M. M. van Paassen, and M. Mulder, "Modeling human difference threshold in perceiving mechanical properties from force," *IEEE Transactions on Human-Machine Systems*, vol. 48, no. 4, pp. 359–368, 2018. DOI: 10.1109/THMS.2018.2844212.

[29] O. Caldiran, H. Tan, and C. Basdogan, "An investigation of haptic perception of viscoelastic materials in the frequency domain," Apr. 2018. DOI: 10.1109/HAPTICS.2018.8357180.

[30] M. Srinivasan, N. Durlach, and G. Beauregard, "The manual resolution of viscosity and mass, die manuelle auflösung von viskosität und masse," in *ASME/DSC, ASME Dynamic Systems and Control Division, 1995, ASME International Mechanical Engineering Congress & Exposition, 1995*, vol. 57-2, New York: American Society of Mechanical Engineers $ASME$; 1995, pp. 657–662, ISBN: 0-7918-1746-6. [Online]. Available: https://www.tib.eu/de/suchen/id/tema%3ATEMAM97026576579.

[31] T. Editors of Encyclopaedia Brittanica, *Friction*, Mar. 2020. [Online]. Available: https://www.britannica.com/science/friction.

[32] G. Ellis, "Chapter 12 - nonlinear behavior and time variation," in *Control System Design Guide (Fourth Edition)*, G. Ellis, Ed., Fourth Edition, Boston: Butterworth-Heinemann, 2012, pp. 235–260, ISBN: 978-0-12-385920-4. DOI: https://doi.org/10.1016/B978-0-12-385920-4.00012-6. [Online]. Available: https://www.sciencedirect.com/science/article/pii/B9780123859204000126.

[33] F. Kingdom and N. Prins, *Psychophysics: A Practical Introduction: Second Edition*. Jan. 2016, pp. 1–331.

[34] W. Fu, M. M. van Paassen, D. A. Abbink, and M. Mulder, "Framework for human haptic perception with delayed force feedback," *IEEE Transactions on Human-Machine Systems*, vol. 49, no. 2, pp. 171–182, 2019. DOI: 10.1109/THMS.2018.2885401.

[35] A. Faul, "G*power 3: A flexible statistical power analysis program for the social, behavioral, and biomedical sciences.," *Behavior research methods.*, vol. 39, no. 2, 2007, ISSN: 1554-351X.